Untersuchung auf Unterschiedliche Rollen von Smad Proteinen in der Signalübertragung der Knochenmorphogenetischen Proteine

Investigation on Distinct Roles of Smad Proteins in Mediating Bone Morphogenetic Proteins Signals

Doctoral thesis for a doctoral degree

at the Graduate School of Life Science

Julius-Maximilians University of Würzburg

Section Biomedicine

submitted by

Gan, Qiang

from

Shaanxi, China

Würzburg, 2011

submitted on: 19. Dec. 2011

(office stamp)

Members of the *Promotionskomitee*:

Chairperson:Thomas Müller

Primary Supervisor: Gregory Harms

Second Supervisor: Manfred Schartl

Third Supervisor: Toni Wagner

Date of Public Defence: 22. May 2012

Acknowledgements

First and foremost, I would like to express my sincere gratitude to Prof. Dr. Gregory S Harms for his supervision, encouragement and support throughout the entire course of my PhD study.

Also, I am very grateful to Prof. Dr. Manfred Schartl and Dr. Toni U Wagner for kind guidance, helpful discussion and valuable advice.

This work would not have been done without the financial support by the German Research Foundation to the Rudolf-Virchow Center for Experimental Biomedicine (DFG Forschungszentrum für Experimentelle Biomedizin).

Part of this work has been done by collaborating with Dr. Soojin Ryu and Boris Knerr, Max-Plank Institute for Medical Research (MPI für Medizinische Forschung) Heidelberg. I wish to thank them for the pleasant collaboration.

I am grateful as well to all the former and present colleagues in the lab for giving me indispensible help, creating a wonderful and fun working environment. Especially, I would like to thank, Mike Friedrich for his readiness with microscopic assistance, Monika Zelman-Femiak for her help and my former colleague Kun Wang for help with a number of plasmid constructs. I also own much thanks to Michael Kraeussling who helped me a lot with zebrafish work.

I appreciate the help from external researchers for sharing me material. I thank Dr. Joerg Wiedenmann for EosFP (Southampton, UK), Prof. Roger Y. Tsien for mCherry (San Diego, USA), Prof. Stephan Sigrist for Dendra2 and for helpful suggestions (Berlin, Germany), Dr. Stephan Kissler for pLB for lentivirus-based knockdown constructs and for helpful suggestions (Würzburg, Germany), Prof. Petra Knaus for C2C12 cell line (Berlin, Germany), PD Dr. Heike Hermanns for HepG2 cell line and Carmen Schäfer for qRT-PCR protocol (Würzburg, Germany), Prof. Paul A. Krieg for pXeX plasmid (Arizona, USA), Dr Geoff Waldo for superfolderGFP (Los Alamos, USA), Prof. John Kuwada for pHSP70-EGFP(HA) (Michigan, USA) , Dr. Özgür Sahin und Dr. Yi Ni for qRT-PCR suggestions (Heidelberg, Germany)

Despite the distance, my parents have always been there for me. My deepest gratitude goes to them for their endless support and constant inspiration through years.

Lastly, I would like to thank my beloved Hui for sharing her memories and experiences with me, for her constant encouragement and understanding, and for always being willing to help me.

Contents

Zusammenfassung

Knochenmorphogenetische Proteine (engl. Bone morphogenetic Proteins, BMPs) sind eine Bestandteil von transforming growth factor-β (TGF-β)-Superfamilie und spielen wichtige Rollen in zahlreichen biologischen Ereignissen in der Entwicklung fast aller mehrzelligen Organismen. Fehlregulierte BMP-Signalweg ist die zugrunde liegenden Ursachen von zahlreichen erblichen und nicht erblichen Krankheiten wie Krebs. Die von BMP induziete breite Palette von biologischen Reaktionen konvergiert auf drei eng verwandten Smad Proteine. Sie vermitteln intrazelluläre Signale von BMP-Rezeptoren in den Zellkern. Die Spezifität des BMP-Signalwegs wurde intensiv auf der Ebene der Ligand-Rezeptor-Wechselwirkungen erforscht, aber, wie die verschiedenen Smad Proteine die durch BMPs hervorgerufen differenziellen Signale beitragen, bleibt unklar.

In dieser Arbeit haben wir die BMP / Smad Signalweg in verschiedenen Aspektenuntersucht. Auf der Suche nach einem geeigneten Fluoreszenz-Reporter im Zebrafisch, verglichen wir verschiedene photo-schaltbaren Proteine und fand EosFP der beste Kandidat für diesen Modellorganismus im Bezug auf seine schnelle Reifung und Fluoreszenz-Intensität.

Wir haben durch molekulare Modifizierung geeignete Vektoren erstellt, die Tol2-Transposon basieren trangenesis im Zebrafisch zu ermöglichen. Damit wurden schließlich transgenzebrafisch-Linien erzeugt. Wir kombinierten Fluoreszenz-Protein-Tagging mit hochauflösender Mikroskopie und untersuchten die Dynamik der Smad-Proteine in Modellsystem Zebrafisch. Es wurde beobachteten, dass Smad5 Kern-Translokation erfährt, als BMP Signalgeber bei Zebrafisch Gastrulation.

Wir erkundeten die Beteiligung der Smad Proteine während der Myogenese-zu-Osteogenese Umwandlung von C2C12 Zelllinie, die durch BMP4 induziert wurde. Mit siRNA versuchten wir die endogene Smad Proteine niederzuschlagen, wobei die Auswirkungen auf diesen gekoppelten noch unterschiedlichen Verfahren durch

quantitative real-time PCR und Terminal-Marker Färbung ausgewertet. Wir spekulieren, dass verschiedene Smad-Komplex Stöchiometrie für unterschiedliche durch BMPs hervorgerufe zelluläre Signale verantwortlich sein könnte.

Summary

Bone morphogenetic proteins (BMPs) belong to the transforming growth factor-β (TGF-β) superfamily and play important roles in numerous biological events in the development of almost all multi-cellular organisms. Dysregulated BMP signaling is the underlying causes of numerous heritable and non-heritable human diseases including cancer. The vast range of biological responses induced by BMPs converges on three closely related Smad proteins that convey intracellular signals from BMP receptors to the nucleus. The specificity of BMP signaling has been intensively investigated at the level of ligand-receptor interactions, but how the different Smad proteins contribute to differential signals elicited by BMPs remains unclear.

In this work, we investigated the BMP/Smad signaling in different aspects. In search for an appropriate fluorescence reporter in zebrafish, we compared different photo-switchable proteins and found EosFP the best candidate this model system for its fast maturation and fluorescence intensity.

We modified and created appropriate vectors enabling Tol2-transposon based trangenesis in zebrafish, with which transgenic zebrafish lines were generated. We combined fluorescence protein tagging with high resolution microscopy and investigate the dynamics of Smad proteins in model system zebrafish. We observed that Smad5 undergoes nucleo-translocation as BMP signal transmitter during zebrafish gastrulation.

We explored the Smad involvement during myogenic-to-osteogenic conversion of C2C12 cell line induced by BMP4. We created transient loss-of-function of Smads by siRNA-mediated knockdowns and analyzed the effects on these coupled yet distinct procedures by quantitative real-time PCR and terminal marker staining. We found that different Smad-complex stoichiometry might be responsible for distinct cellular signals elicited by BMPs.

1 Introduction

1.1 Background

Bone morphogenetic proteins (BMPs) are a group of phylogeneticlly conserved growth factors. With more than 20 members identified to date, they belong to and constitute the largest subfamily of the transforming growth factor-β (TGF-β) superfamily (Hogan, 1996). Since the first identification of the bone-inducing activity in the 1960s (Urist, 1965), novel functions of BMPs have been investigated and they have been found to play indispensable roles in development of numerous multiple-cellular organisms (Chen et al, 2004; Hogan, 1996). Accordingly, malfunction of BMP/Smad signaling is frequently accompanied by heritable and/or non-heritable human diseases including cancer (Harradine & Akhurst, 2006; Singh & Morris, 2010; Thawani et al, 2010). Increased attention has also been drawn to roles of BMPs in regulating fate choices during stem cell differentiation recently (Varga & Wrana, 2005; Watabe & Miyazono, 2009).

The signals originate from a variety of secreted BMP ligands, which recruit and activate membrane-anchored receptors of target cells. The signals elicited by BMPs are believed to be mainly mediated by a family of highly conserved intercellular transmitters, namely Smad proteins in numerous multi-cellular organisms from fruitfly to human (Massague et al, 2005). To date, eight different Smads have been identified in mammals, six of them participate BMP-directed signaling. According to their roles, these Smad proteins are further classified as receptor-regulated Smads (R-Smads), common Smad (Co-Smad) and inhibitory Smads (I-Smads) (Feng & Derynck, 2005).

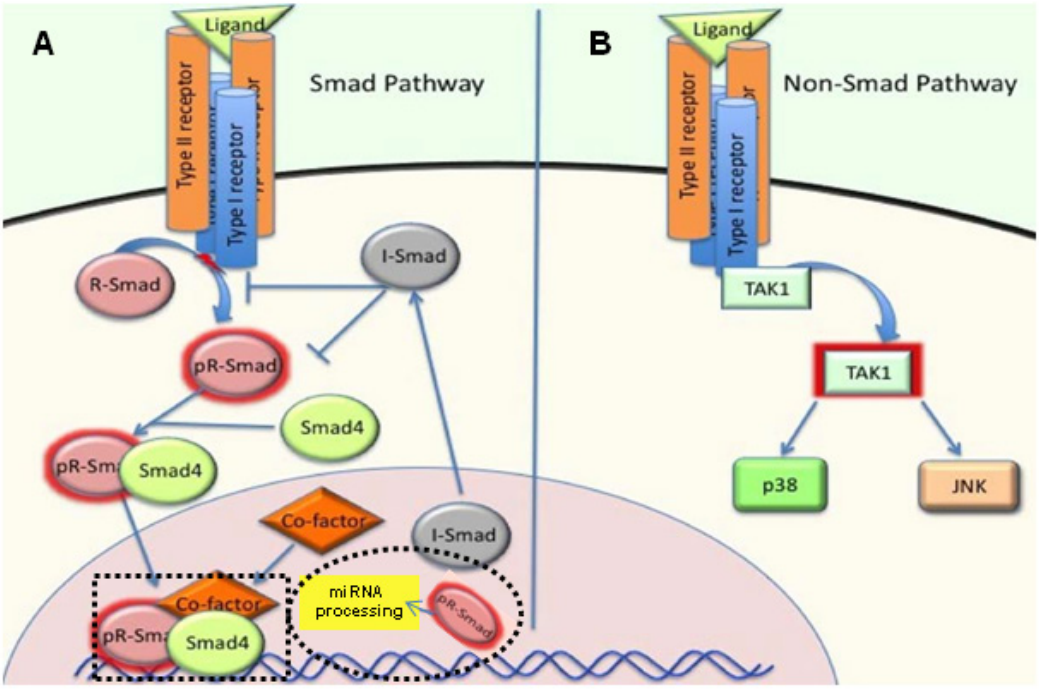

Figure 1: BMP-directed intracellular signaling pathways. Signals elicited by BMPs are transduced by membrane receptors, which in turn activate distinct intracellular transmitters. (A) Smad proteins transduce BMPs signal as transcription factors (rectangle) and/or as microRNA processors (oval). (B) BMPs signals are mediated by p38 and/or JNK. Modified from (Song et al, 2009)

The R-Smads are phosphorylated at their C-terminal SSXS motif upon ligand-induced receptor activation. They form complex with the common Smad (Co-Smad), Smad4, and enter the nucleus where they act as transcription factors to regulate gene expression. The Smad6 and Smad7 counteract the above described Smad signaling by interfering in the receptor-mediated phosphorylation and/or formation of R-Smad/Co-Smad complexes (Feng & Derynck, 2005; Heldin et al, 1997; Massague et al, 2005; Schmierer & Hill, 2007). In such a "canonical" BMP/Smad signaling, the Smad-complex acts as a transcription factor to regulate gene expression in presence or absence other cofactors (Figure 1A, dotted rectangle) (Feng & Derynck, 2005; Heldin et al, 1997; Massague et al, 2005; Schmierer & Hill, 2007). Activated R-Smads alone have also been described to have microRNA-processing activity (Figure 1A, dotted oval) (Davis-Dusenbery & Hata,

2011; Davis et al, 2008; Song et al, 2009). Recent studies on BMPs' function have revealed that BMPs can also activate other downsteam effectors besides Smad proteins, such as JNK, p38 and so on (Figure 1B) (Derynck & Zhang, 2003; Song et al, 2009). However, such "non-Smad" BMP signaling was beyond the scope and objectives of this study.

To date, three R-Smads have been identified that mediate BMP signaling in mammalian cells (BR-Smads), namely Smad1, Smad5 and Smad8 (known also as Smad9). Although their highly conserved amino acid sequences imply possible functional interchangeability, differences amongst these three intracellular signal transmitters have not been fully characterized (Miyazono et al, 2010). For instance, Smad1 and Smad5 are expressed at different time points and shown in Figure 2A, where Smad5 is maternally expressed whereas Smad1's expression is zygotic (Dick et al, 1999). Even when both transcripts are present, they were found to be localized at different embryo areas (Figure 2B) (Maegawa et al, 2006).

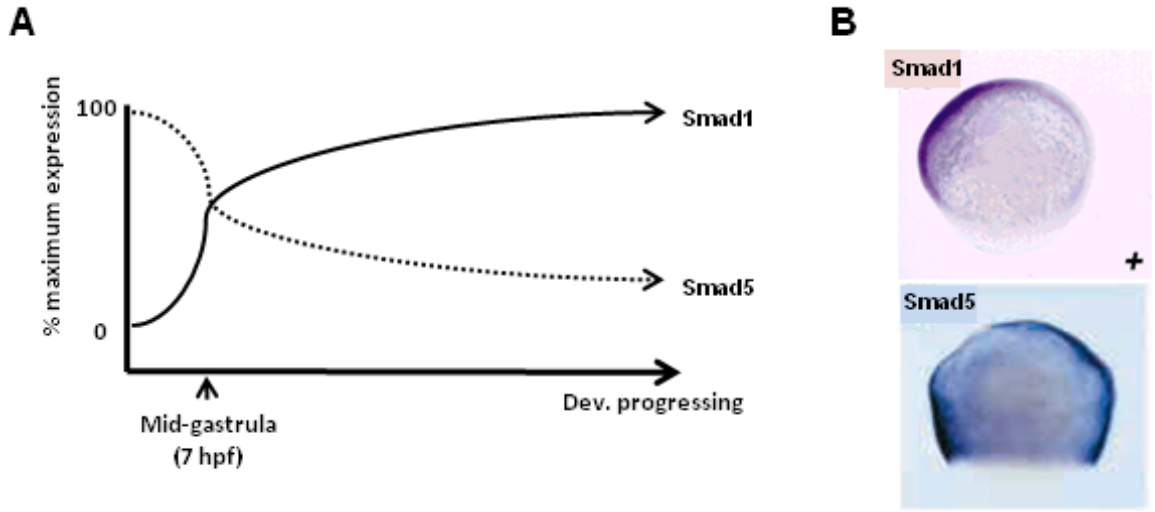

Figure 2: Spatiotemporal expression of Smad1 and Smad5 in early zebrafish development. (A) Temporal expression of Smad1 (solid line) and Smad5 (dotted line) transcripts. Diagram is drawn based on the results from (Dick et al, 1999). (B) Spatial localization of Smad1 and Smad5 transcripts, lateral view with dorsal right at 70% epiboly of zebrafish embryo. Modified from (Maegawa et al, 2006).

Forced expression and morpholino-mediated knockdown of Smad1 and Smad5 resulted in dissimilar phenotype in zebrafish (Dick et al, 1999; McReynolds et al, 2007). However, overlapping developmental abnormalities have been observed in knockout mice (Arnold et al, 2006; Chang et al, 1999; Pangas et al, 2008; Tremblay et al, 2001). Moreover, there has been evidence that different downstream gene pools were subject to the loss of Smad in zebrafish. As shown in Figure 3A, individual knockdowns of either Smad1 or Smad5 alone led to up-regulation of 702 or 542 downstream genes assayed with 160 genes in common. Meanwhile, 718 genes in case of Smad1 knockdown and 461 genes in case of Smad5 knockdown were shown down-regulated. Thus, among these down-regulated genes, many unique genes were correlated to BMP signaling for Smad5 while many unique genes in Smad1 knockdown were less likely to be considered as BMP-relevant judged by a system biology approach (Figure 3B) (McReynolds et al, 2007). Therefore, the central aim of this research is to investigate the functional differences among these Smads as BMP-signal transmitters.

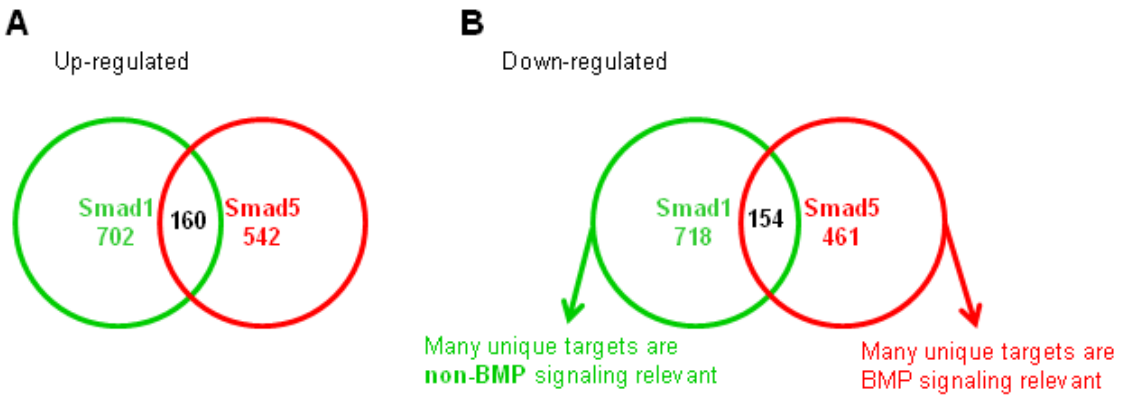

Figure 3: Sets of genes affected in loss of Smads. (A) Genes up-regulated in Smad1 (green) and Smad5 (red) knockdowns; (B) Genes down-regulated in Smad1 (green) and Smad5 (red) knockdowns. Diagram is drawn based on results from (McReynolds et al, 2007).

1.2 Aims of the study

As BMP/Smad signaling is essential for vertebrate development, forward genetic investigation with Smad knockout approaches have been largely restricted because of embryonic lethality (Arnold et al, 2006; Chang et al, 1999; Dick et al, 1999). Although there have been functional studies with over-expression and knockdowns of Smad *in vivo* as mentioned above, the results seem rather complicated (Arnold et al, 2006; Chang et al, 1999; Dick et al, 1999; McReynolds et al, 2007). We argue that due to the contextual complexity of *in vivo* settings and the multi-functional properties of BMP/Smad signaling itself, individual Smad proteins have been difficult to assign and interpret to defined biological processes.

Some studies took advantage of phospho-antibodies to investigate the activation of Smad proteins (Tucker et al, 2008). Since all R-Smads have conserved sequence, especially at the extreme C-terminus where receptor-directed phosphorylation takes place, there has not been reported for an antibody being able to recognize both phosphate-groups and specifically different Smad proteins.

We were interested in the spatiotemporal activation of different Smad proteins in the model system of the zebrafish. Modern recombinant DNA technique allows the creation of fluorescence protein (FP) tagged Smad fusions, which enable us to distinguish different Smad proteins (Yuste, 2005). High resolution microscopy in combination with zebrafish will make the *in vivo* imaging possible, because of its fast external development and transparency (Beis & Stainier, 2006; Keller et al, 2008). Therefore, we intend to investigate the spatiotemporal activation of this signaling with high resolution microscopy using zebrafish as model system.

The blueprint summarized in Figure 4 is based on availability of an appropriate fluorescent biosensor, which will be introduced and explained in section 3.1 and section 3.2.

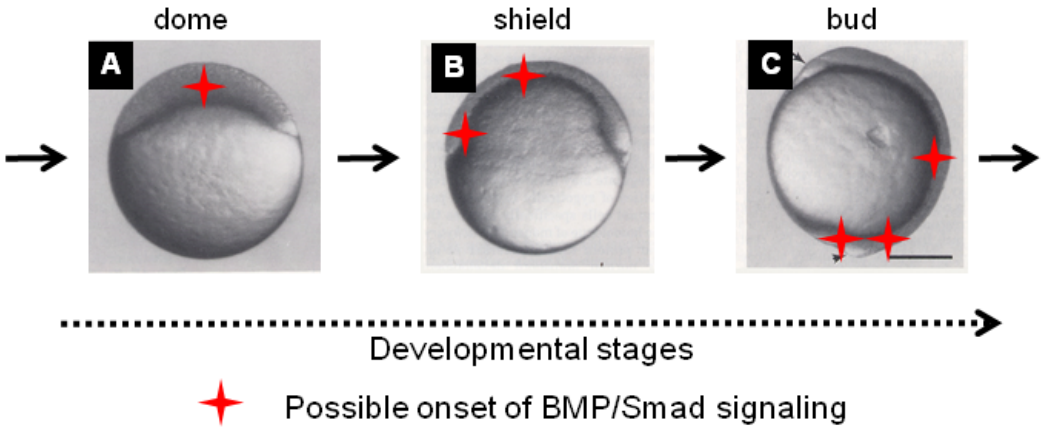

Figure 4: Schematic diagram of spatiotemporal BMP/Smad activation during zebrafish embryogenesis. (A) An initial positive signal detected by the biosensor at a given developmental stage is marked as a red star. (B, C) During the development more signals will be detected as red stars. The relative later signals could be at the same area (ripple signal). Modified from (Kimmel et al, 1995).

With the aid of an appropriate biosensor, the activation of BMP/Smad signaling will give a fluorescent signal which is recorded by a microscope along the fish development in real time (Figure 4, red stars). For instance, as it has been shown that endogenous BMP2 begins to be expressed at onset of blastulation (Thisse et al, 2004), we will be able to detect a positive signal and its progressing between dome and shield stages of development (Figure 4A, B). Such a profile of BMP/Smad signaling activation is suggested to provide a better understanding of this pathway in the patterning of the dorsal-ventral body axis parallel to the involvement of individual Smad proteins as BMP-signal transmitters.

Microscopy has been employed as a powerful tool since almost the birth of modern biology when Leeuwenhoek reported the discovery of micro-organisms in 1676 (Wootton, 2006). Recently, it has been reported to be possible to image live zebrafish embryo *in toto* as it develops (Keller et al, 2008; Keller et al, 2011).

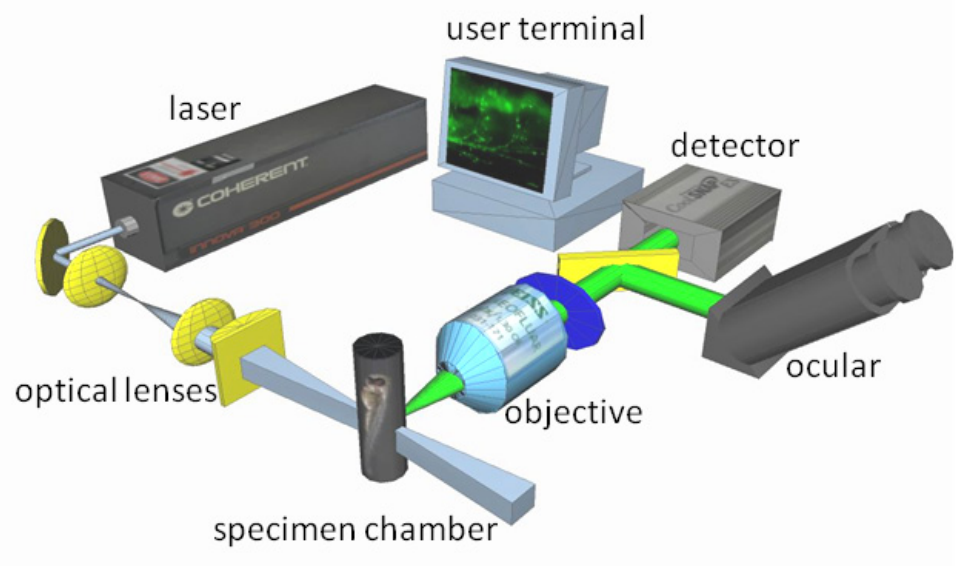

Figure 5: Schematic diagram of a home-made SPIM. Diagram is from (Friedrich, 2009).

To visualize the transparent embryo of fish, we will apply the selective plane illumination microscopy (SPIM). Figure 5 shows the setup of our home-made SPIM. The highlights of this microscopy are: (1) By combination of a pair of telescope lense and a cylinderic lense, it will generate a thin sheet light of high power capable of penetrating the specimen of mm scales. (2) The detector position at a 90° angle to the illumination sheet minimizes the out of focus fluorescence. Applying this newly developed microscopic technique, we could achieve to observe the zebrafish embryo at confocal microscopy resolution but at rates much faster than confocal microscopy and applicable to development.

2 Materials and Methods

2.1 Molecular Cloning and Enzymes

Enzymes — restriction enzymes, polymerases, ligases and so on — were purchased from New England Biolabs. MACHEREY-NAGEL kits were used for nucleic acid isolation and extraction. Standard procedures for molecular cloning such as plasmid construction, bacterial transformation and so on were performed with reference from "Molecular Cloning-a laboratory Manual" (Sambrook & Russell, 2006) or after enzyme suppliers' instructions.

2.2 Antibodies

For immuno-staining:

GFP Mouse mAb (Abcam, 1:200), human Myosin heavy chain Mouse mAb (R&D SYSTEMS, 1:200), phospho-Smad1/5/8 Rabbit pAb (Cell Signaling Technology, 1:100), anti-Rabbit Alexa568 (Molecular Probe, 1:500), anti-Mouse Alexa488 (Molecular Probe, 1:500), Hoechst (Molecular Probe, 1:10,000)

For immuno-blotting:

GAPDH Rabbit mAb (Cell Signaling Technology, 1:1500), Smad1 Rabbit pAb (Cell Signaling Technology, 1:1000), Smad4 Rabbit pAb (Cell Signaling Technology, 1:1000), Smad5 Rabbit mAb (Epitomics, 1:1500), Smad8 Goat pAb (IMGENEX, 1:800), anti-Rabbit IRDye®800CW (LI-COR, 1:10,000), anti-Goat IRDye®800CW (LI-COR, 1:10,000)

2.3 Genetic modified organisms

Table 1 lists the bacterial strains, cell lines and fish strains used in this work with source and/or reference.

Table 1 Organisms used in this work

Strain	Application	Reference or source
E. coli DH5α	Plasmids Construction	New England Biolabs, (Taylor et al, 1993)
E. coli BL21(DE3)	Inducible expression in *E. coli*	Lab Caroline Kisker in RVZ, (Studier & Moffatt, 1986)
Human embryonic kidney (HEK)	*In vitro* analysis	ATCC CRL-1573, (Graham et al, 1977)
Mouse (C2C12)	*In vitro* analysis	Lab Petra Knaus, FU Berlin, (Yaffe & Saxel, 1977)
Zebrafish (TÜ)	*In vivo* analysis	Lab Manfred Schartl, Uni Würzburg
Zebrafish (AB/TL)	*In vivo* analysis	Lab Soojin Ryu, MPI for medical research Heidelberg, (Baba et al, 2006)

2.4 Fluorescent proteins

Table 2 lists the fluorescent proteins used in this work with source and/or reference.

Table 2 Fluorescent proteins used in this work

Fluorescent proteins	Spectrum	Source, Reference
eGFP	green	Clontech, (Cormack et al, 1996)
EBFP2	blue	Lab Manfred Schartl, Uni Würzburg, (Ai et al, 2007)
mCherry	red	Lab Roger Tsien, UCSD, (Shaner et al, 2004)
EosFP	green-to-red	Lab Jörg Wiedenmann, Uni Ulm, (Wiedenmann et al, 2004)
Kaeda	green-to-red	MBL, (Ando et al, 2002)
Dendra2	green-to-red	Lab Stephan Sigrist, FU Berlin, (Baba et al, 2006; Gurskaya et al, 2006)

2.5 Experimental methods

2.5.1 Construction of eukaryotic expression vector with N-terminal monomeric enhanced green fluorescent protein fusion

The monomeric version (A206K) of enhanced green fluorescent protein (meGFP) was made by PCR-based mutation using pEGFP-N1 (Clontech) as template (Cormack et al, 1996; Zacharias et al, 2002). The meGFP fragment was cloned into pcDNA3.1 (+) (Invitrogen) to create an N-terminal tag expression vector.

2.5.2 Cloning murine Smad1, Smad4, Smad5, Smad8 and construction of expression vectors with GFP tag

Total RNAs were extracted from C2C12 cells with RNeasy Mini Kit (Qiagen), reverse-transcribed with RevertAid™ First Strand cDNA Synthesis Kit (Fermentas) using isolated total RNA as template and oligo-dT as primer. Mouse full-length cDNAs encoding Smad1, Smad4, Smad5 and Smad8 were all amplified with 21-bp gene specific primer-pairs flanking 5'- and 3'- targeted sequence based on the mouse Smad (mSmad) mRNA entries in NCBI Genbank. mSmad1 (NM_008539.3), mSmad4 (NM_008540.2), mSmad5 (NM_008541.3) and mSmad8 (NM_019483.4). The resulting mouse full-length Smad cDNAs were sub-cloned into the expression vector described in section 2.5.1.

2.5.3 *In vitro* transcription, micro-injection of zebrafish embryo for transient expression and stable transgenic lines

Plasmids were linearized by cutting with appropriate restriction enzyme right after the coding sequence and purified by phenol/chloroform extraction. 1μg DNA was reverse-transcribed to mRNA *in vitro* with the mScript™ mRNA Production System (EPICENTRE via Biozym GmbH) enabling 5'-capping and 3'-polyA tailing after manufacturer's instruction. The resulting transcript was extracted and dissolved in nuclease-free water (Qiagen). For transient expression, 100 ng purified *in vitro* transcribed mRNA was microinjected into zebrafish embryo at 1-4 cell stage. For stable

transgenic fish lines, 20 ng Tol2 mRNA and 100 ng plasmid DNA were microinjected into zebrafish embryo at 1-4 cell stage. Zebrafish embryos were incubated at 27-28° C for growth.

2.5.4 Cell culture, transfection and RNA interference

HEK293 and C2C12 cells were maintained and propagated in growth medium (GM) of DMEM (Sigma-Aldrich) containing 10% FBS (PAA) and 1% Penicillin-Streptomycin (Sigma-Aldrich) at 37°C with 5% or 10% CO_2. Transfection of plasmid DNA was performed with Attractene transfection reagent (Qiagen). Transfection of short interference RNAs (siRNAs) was performed with Hiperfect transfection reagent (Qiagen). Negative control (NC) siRNA targeting none of endogenous transcript (AllStars Neg. siRNA) and FlexiTube GeneSolution siRNAs specific to mouse Smad1, Smad4, Smad5 and Smad8 were purchased from Qiagen GmbH, Germany. The following siRNAs were applied to silence each Smad throughout this work: mSmad1 (SI00177072, S1), mSmad4 (SI01426215, S4), mSmad5 (SI00177100, S5), mSmad8 (SI01426243, S8). NC and gene specific siRNAs were used at a concentration of 7.5 nM without exception.

2.5.5 *In vitro* differentiation

In vitro differentiation was performed as previously described (Blau et al, 1985; Katagiri et al, 1994). Briefly, sub-confluent C2C12 cells grown in GM were re-cultured in differentiation medium (DM) where FBS is replaced with 2% horse serum (Sigma-Aldrich) on day 1 and medium was replaced every day. Cells were treated with BMP in DM for 3 hours and medium was replaced with DM on day 1 for myogenic inhibition or always with BMP-4 (5 ng/ml, Sigma-Aldrich) in DM since day 1 for osteogenic induction. On day 4, cells were fixed and stained against myosin heavy chain for myogenic differentiation or stained in substrate solution prepared from ready-to-use NBT/BCIP tablet (Roche Diagnostics) for 1 hour at room temperature in the dark for ALP activity.

2.5.6 Smad phosphorylation and nucleo-translocation

Cells were seeded and grown on glass coverslips in GM. 24 hours post transfection, cells were starved in GM containing 0.2% FBS for 16 hours, treated with or without 5 ng/ml BMP-4 for 1 hour and immuno-stained against GFP and p-Smad antibodies.

2.5.7 Immuno-staining and imaging

For immuno-staining, cells on coverslips were fixed in 3% PFA/PBS, permeablized with 0.2% Tx-100/PBS, blocked and incubated in 2% BSA/PBS with primary antibody, followed by fluorescence coupled secondary antibody and Hoechst staining. The prepared coverslips were imaged on a Leica TCS SP5 confocal microscope.

2.5.8 RNA extraction and quantitative reverse transcriptase (RT)-PCR

Total RNA was extracted from (treated) cells using an RNeasy Mini kit (Qiagen) and cDNAs were synthesized using a QuantiTect Rev. Transcription Kit with Oligo-dT/random-hexomer primer mix (Qiagen) after manufacturer's instruction. 10 µl reaction volume for kinetic real-time PCR was prepared using 2.5 ng cDNA template, 300 nM primer pairs with 2x KAPA SYBR Fast qPCR Master mix (PEQLAB) on a QIAgility robot (Qiagen). The reactions were performed on an ABI 7900HT (Applied Biosystems) with a 3-step cycling protocol for 40 cycles (initial anneal and enzyme activation at 95 °C for 5 min, anneal and elongate at 60 °C for 30 sec, denature at 95 °C for 10 sec). Specificity of primers was verified by dissociation/melting curve. Primers used for PCRs were designed using web-based resources PrimerBank (Spandidos et al, 2010) and Primer3 (Rozen & Skaletsky, 2000). Their sequences are listed in Table 3. The mRNA levels of genes of interest were normalized to glyceraldehyd-3-phosphat-dehydrogenase (GAPDH) and plotted against a reference gene or against the maximum of its own expression at different time-points.

Table 3 Primers for qRT-PCR

Gene Symbol Acc. Nr.	Primer Sources (Amplicon bp)	Sequence (5' -> 3')
mSmad1 NM_008539	PrimerBank 31543220a1 (147)	Fwd:GCTTCGTGAAGGGTTGGGG Rev:CGGATGAAATAGGATTGTGGGG
mSmad4 NM_008540	PrimerBank 31543223b2 (110)	Fwd:AGGTGGCCTGATCTACACAAG Rev:ACCCGCTCATAGTGATATGGATT
mSmad5 NM_008541	PrimerBank 6678774a1 (114)	Fwd:TTGTTCAGAGTAGGAACTGCAAC Rev:GAAGCTGAGCAAACTCCTGAT
mSmad8 NM_019483	Primer3 (96)	Fwd:CGGGTCAGCCTAGCAAGTG Rev:GAGCCGAACGGGAACTCAC
mGAPDH NM_008084	PrimerBank 6679937a1 (123)	Fwd:AGGTCGGTGTGAACGGATTTG Rev:TGTAGACCATGTAGTTGAGGTCA
mRunx2 NM_001146038	PrimerBank 225690525b1 (84)	Fwd:GACTGTGGTTACCGTCATGGC Rev:ACTTGGTTTTTCATAACAGCGGA
mDlx3 NM_010055	Primer3 (85)	Fwd:TATTACAGCGCTCCTCAGCAT Rev:TGAACTGGTGGTGGTAGGTGT
mOsx(Sp7) NM_130458	PrimerBank 18485518a1 (156)	Fwd:ATGGCGTCCTCTCTGCTTG Rev:TGAAAGGTCAGCGTATGGCTT
mOcn(mBglap) NM_031368	PrimerBank 13811695a1 (187)	Fwd:CTGACCTCACAGATGCCAAGC Rev:TGGTCTGATAGCTCGTCACAAG
mMyoD NM_010866	PrimerBank 170172578b2 (119)	Fwd:ATGATGACCCGTGTTTCGACT Rev:CACCGCAGTAGGGAAGTGT
mMyoG NM_031189	PrimerBank 13654247a1 (106)	Fwd:GAGACATCCCCCTATTTCTACCA Rev:GCTCAGTCCGCTCATAGCC

2.5.9 Cell lysis, immuno-blotting and documentation

Cells were harvested, lysed in CelLytic™M Cell Lysis Reagent (Sigma-Aldrich) supplemented with Protease Inhibitor Cocktail (Sigma-Aldrich). The cell-lysate was

analyzed by SDS PAGE followed by immune-blotting. Li-COR Odyssey Blocking Buffer and IRDye®-coupled secondary antibodies were applied and stained nitrocellular membrane was scanned with a LI-COR Odyssey Imaging System (LI-COR).

2.5.10 Zebrafish embryo imaging

(Micro-injected) zebrafish embryos were sorted for viability and for fluorescence under a bench fluorescence microscope. Positive embryos were mounted in 1% agarose gel for SPIM real-time imaging or stained in advance for confocal imaging. Images were recorded and analyzed with the NIH ImageJ Program (Collins, 2007).

2.5.11 Imaging processing and diagrammatic documentation

Images recorded with confocal microscope and with Odyssey system were analyzed and processed with the NIH ImageJ Program (Collins, 2007). Diagrams of enumerated results were created with the KaleidaGraph software (Synergy Software).

3 Results and Discussions

3.1 Spatiotemporal visualization of bone morphogenetic proteins gradient *in vivo*

To gain better insight about the spatiotemporal activation of BMP/Smad signaling, we created a biosensor based on a fluorescent protein (FP) with a BMP-responsive DNA cis-element regulation. Once target cells receive extracellular BMP ligands, the signals should be transduced by membrane receptors, which in turn will phosphorylate downstream Smad effectors. The activated Smads then enter nucleus and function as transcription factors to regulate numerous downstream gene expression.

We desired a fluorescent reporter to not only give a signal response but to also reflect the dynamic timing change of the signal. A class of fluorescent proteins, namely photo-switchable fluorescent proteins (psFPs), meets our demand. As depicted in Figure 6, EosFP normally emits green. UV-irradiation causes the break of the intrinsic peptide bond and the protein emits then red.

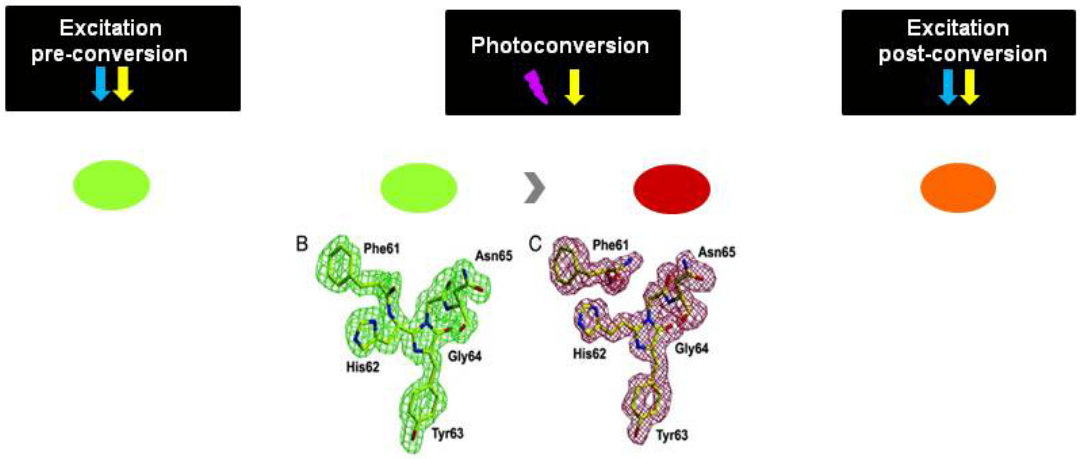

Figure 6: Green-to-red photo-conversion of a photo-switchable fluorescent protein EosFP. EosFP is routinely excited by a 488 nm laser and emits as a green fluorescent protein. The peptide bond between Phe61 and His62 is readlily broken upon UV-irradiation. This

results a red emission of the protein when it is excited by a 594 nm laser. The structure is from (Wiedenmann et al, 2004)

When such constructs are introduced *in vivo* in zebrafish as in this study, it will be possible to visualize the activation of BMP/Smad signaling in zebrafish development.

To enable the *in toto* real-time imaging, we applied the SPIM. In this newly developed technique, a strong yet thin light sheet is created by a series of well-set optical lenses as shown in Figure 5. This allows illumination of the biological sample positioned in the chamber to be well controlled so that only the section for data acquisition is scanned while the other part of the sample is not. This is plausible for long-term imaging with fluorescent protein because long intensive illumination leads to photo-bleaching of the proteins.

To make such a biosensor, we need to have the fluorescent protein reporter under a BMP-responsive *cis*-element as shown in Figure 7. In contrast to the CMV promoter where the reporter is constitutively expressed, the BMP-inducible *cis*-element is supposed to drive the expression of reporter when the signaling is set on.

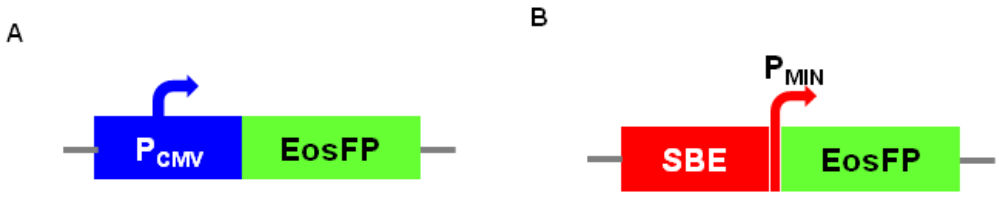

Figure 7: Biosensor for BMP signal detection. (A) EosFP is under CMV promoter and is constitutively expressed. (B) EosFP is under Smad-binding element, a characterized *cis*-element that enables detection of Smad activation.

When such a biosensor is introduced into zebrafish, we are able to track the dynamic BMP signaling. For instance, when BMP signal is on at a given stage, a signal will be recorded as the emission of the reporter Fluorescent protein (Figure 8A). This signal can

be photo-converted from green to red by focal UV-irradiation (Figure 8B). The fish undergoes further development and new foci of BMP signal will once again be recorded as newly green emission (Figure 8C).

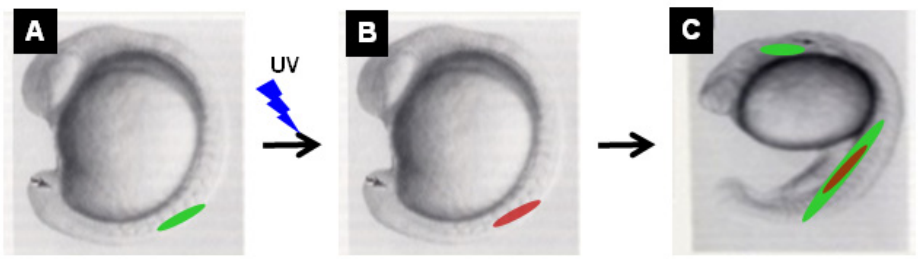

Figure 8: FP-Biosensor for BMP signal detection in zebrafish. (A, B) BMP signal detected at one time point was recorded as green fluorescence signal, which is photo-converted to red by UV-irradiation. (C) Late activation of BMP signal is recorded as green and is readily distinguishable to the former red signal.

3.1.1 Creation of an inducible expression vector

To be able to assay a suitable fluorescent protein as for the reporter, we modified an IPTG-inducible expression vector pTYB1 from New England Biolabs to replace the intein tag with a multiple cloning sites, where FPs could be cloned (Figure 9). The resulting pTYB1Δ plasmid -- when introduced into an *E. coli* BL21(DE3) strain, which constitutively expresses T7 RNA polymerase -- will allow the expression of cloned FPs upon addition of Isopropyl-β-D-thiogalactopyranosid (IPTG), a lac repressor competitor.

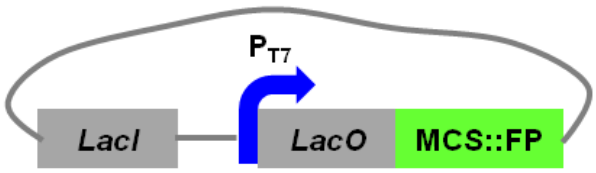

Figure 9: Expression vector pTYB1 Δ constructed to screen different psFPs. BMP-directed intracellular signaling pathways. Signals elicited by BMPs are transduced by membrane receptors, which in turn activate distinct intracellular transmitters.

Three photo-switchable fluorescent proteins, namely Dendra2, Kaede and EosFP together

with eGFP as reference were PCR-amplified and cloned onto this vector. The resulting plasmids were used to transform the *E. coli* BL21 (DE3) cells to assay their performance in terms of folding dynamics. Table 4 summarizes the constructs made to search for a best photo-switchable fluorescent protein as a reporter.

Table 4 Constructs for psFP assays

Plasmid	Property	Purpose
pTYB1	pTYB1 with intein tag insert	Overexpression in *E. coli* BL21(DE3), NEB #E6901
pTYB1Δ	pTYB1 MCS::intein	Parental plasmid for psFP cloning
pTYB1ΔeGFP	pTYB1 MCS::eGFP	Overexpression eGFP
pTYB1ΔEosFP	pTYB1 MCS::EosFP	Overexpression EosFP
pTYB1ΔKaede	pTYB1 MCS::Kaede	Overexpression Kaede
pTYB1ΔDendra2	pTYB1 MCS::Dendra2	Overexpression Dendra2

3.1.2 Screening on fluorescent proteins for an appropriate reporter for zebrafish

We then assayed the different properties of the photo-switchable fluorescent proteins (psFPs). *E. coli* clones bearing different vectors were inoculated and incubated for overnight at 37°C in LB medium containing antibiotic. Dilution was made from the overnight culture to synchronize the growth of different clones. When the cultures reached mid-exponential phase with an optical density (OD_{600}) about 0.5, 1mM IPTG was added to the culture and the temperature for incubation was changed to 28°C to be consistent with the standard zebrafish growth temperature. Cells were harvested after different induction time and concentrated by centrifugation of 1 ml culture and resuspension in 100 µl PBS. Cells were allowed to evenly attach on a 5 mm square thin agarose sheet on a coverslip prepared in advance. The prepared glass coverslips were subject to confocal microscopy to detect the fluorescence of individual FPs.

As shown in Figure 10, induced expression of all FPs was detected, indicating the induction system functioned. The EosFP ranked top because significant fluorescence was

already detected by 25 minutes induction (Figure 10C). By 50 minutes, expression of Kaede was also detected, albeit notably less significant than EosFP (Figure 10, compare G and H). A very slight expression of eGFP and Dendra2 was detected even till 100 minutes after induction under same condition (Figure 10A, B, E, F, I, J).

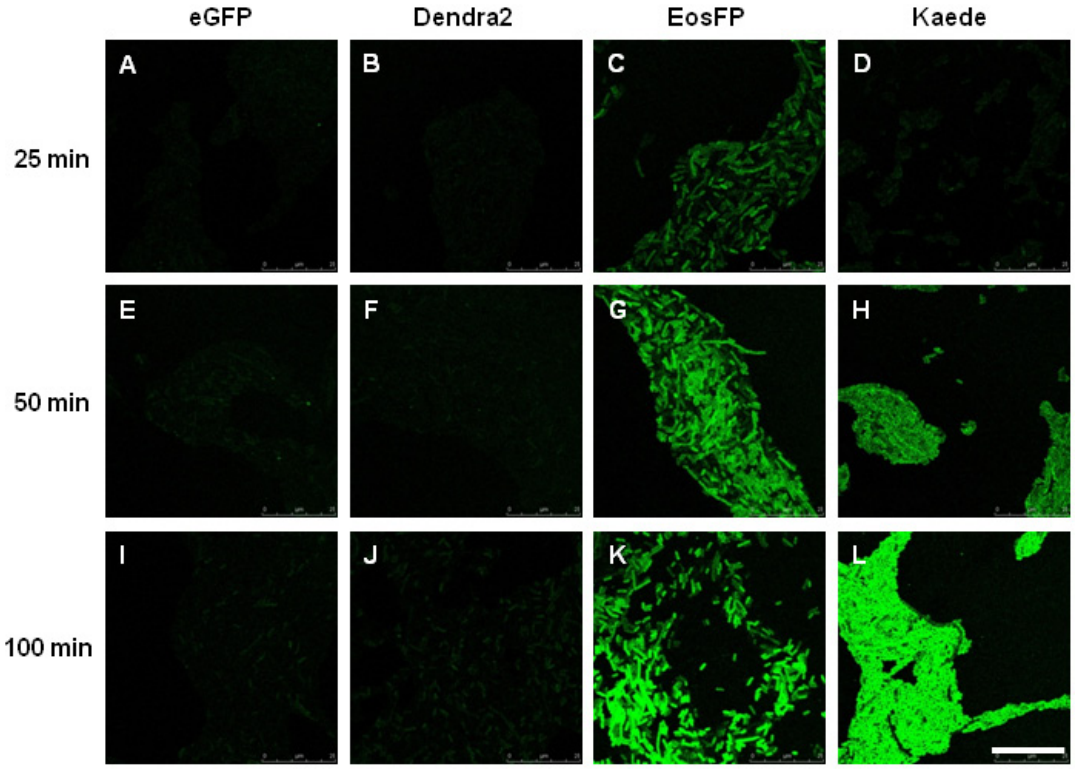

Figure 10: Expression of psFP candidates in bacteria. Dendra2 (B, F, J), EosFP (C, G, K) and Kaede (D, H, L) were induced to express in bacteria upon IPTG. Fluorescence of each FP was assayed 25 min, 50 min and 100 min after induction.

Assuming that the induction of all clones was comparable, which means that almost same amount of mRNA was present, the fluorescence detected with each fluorescent protein was theoretically directly related to their intrinsic maturation/folding dynamics. Therefore, due to its fastest maturation at 28°C, EosFP was considered as the best reporter FP and suitable for our intended study in zebrafish.

3.1.3 Optimization of the photo-conversion of EosFP

One of the highlights of EosFP is its photo-activable switch of emission from green to red. We tried to create a suitable protocol to perform such process with our home-made SPIM

setup. EosFP was firstly re-cloned onto pcDNA3.1(+) vector after T7 promoter. The resulting plasmid was linearized and *in vitro* transcribed. The resulting mRNA coding EosFP was micro-injected into 1-cell stage of zebrafish embryos. The injected embryos were sorted for green fluorescence under stereomicroscope about 5-6 hours post fertilization. Positive embryos were imbedded in 1% agarose in tube and imaged with SPIM.

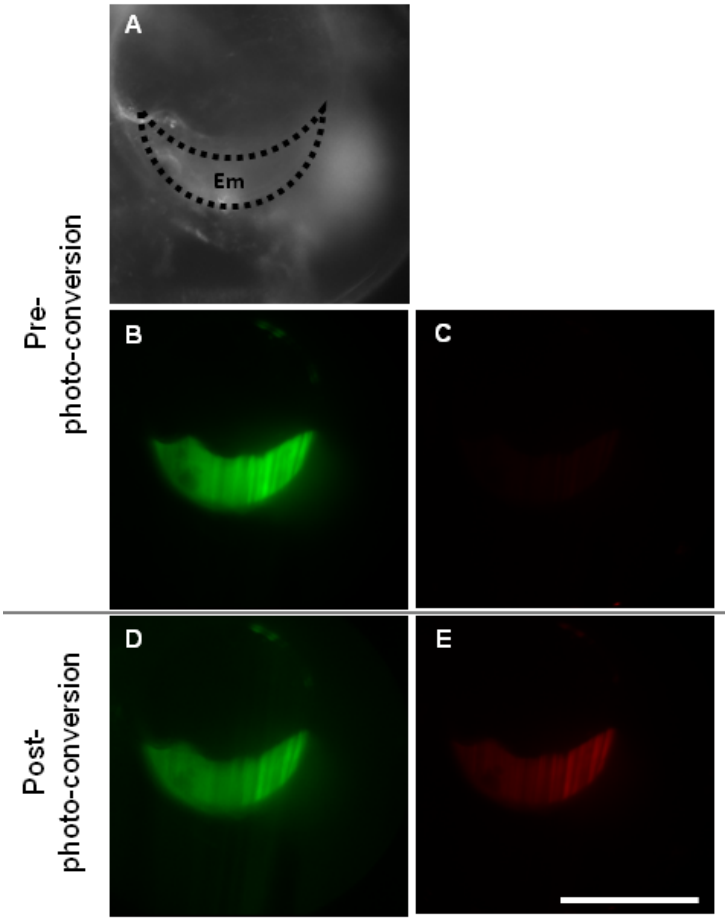

Figure 11: Green-to-red photoconversion of EosFP in zebrafish embryo detected by SPIM. *In vitro* synthesized EosFP mRNA was micro-injected into 1-cell stage of zebrafish embryos. 6 hours post fertilization, fluorescent embryos were imaged under home-made SPIM. (A) Transmission view of the embryo highlighted as Em inside of dotted line area. (B, C) The embryo was illuminate with both 488 nm and 561 nm lasers while only green fluorescence was observed. (D, E) After UV-irradiation, the embryo was again illuminated with both lasers and fluorescence in both green and red channels were observed. Bar 200 µm.

As shown in Figure 11, only green fluorescence was initially detected when EosFP was translated *in vivo* (Figure 11B, C). The fluorescence underwent a green-to-red conversion after UV-irradiation (Figure 11D, E), indicating an UV-induced photo-convertion had taken place.

3.1.4 Creation of BMP-responsive reporter with EosFP

A Smad-binding element (SBE) (Jonk et al, 1998) with a minimal promoter from pGL4 (Promega) were PCR-amplified and cloned right in front of EosFP coding sequence on pcDNA3.1 (+) vector.

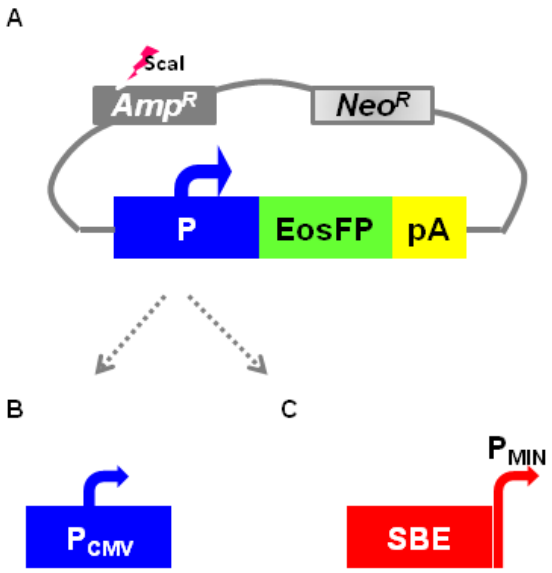

Figure 12: Creation of BMP-responsive reporter with EosFP. (A, B) The constitutively expressing CMV promoter in pcDNA3.1(+). (C) Promoter was replaced by a Smad-binding element supplemented with a minimal promoter.

The plasmids were linearized by cutting with restriction enzyme ScaI within ampicillin resistance gene. The resulting linearized plasmids were transfected into a BMP-sensitive cell line C2C12. After 2 weeks selection of the transfected cell lines in growth medium containing G418, stable cell lines from neomycin-resistant colonies were established.

We then test the reporter constructs upon BMP stimulation. Stable C2C12 cell lines

bearing the SBE-EosFP or CMV-EosFP constructs were kept in growth medium containing G418 for selection. BMP-2 was added to the cells bearing BMP-responsive reporter.

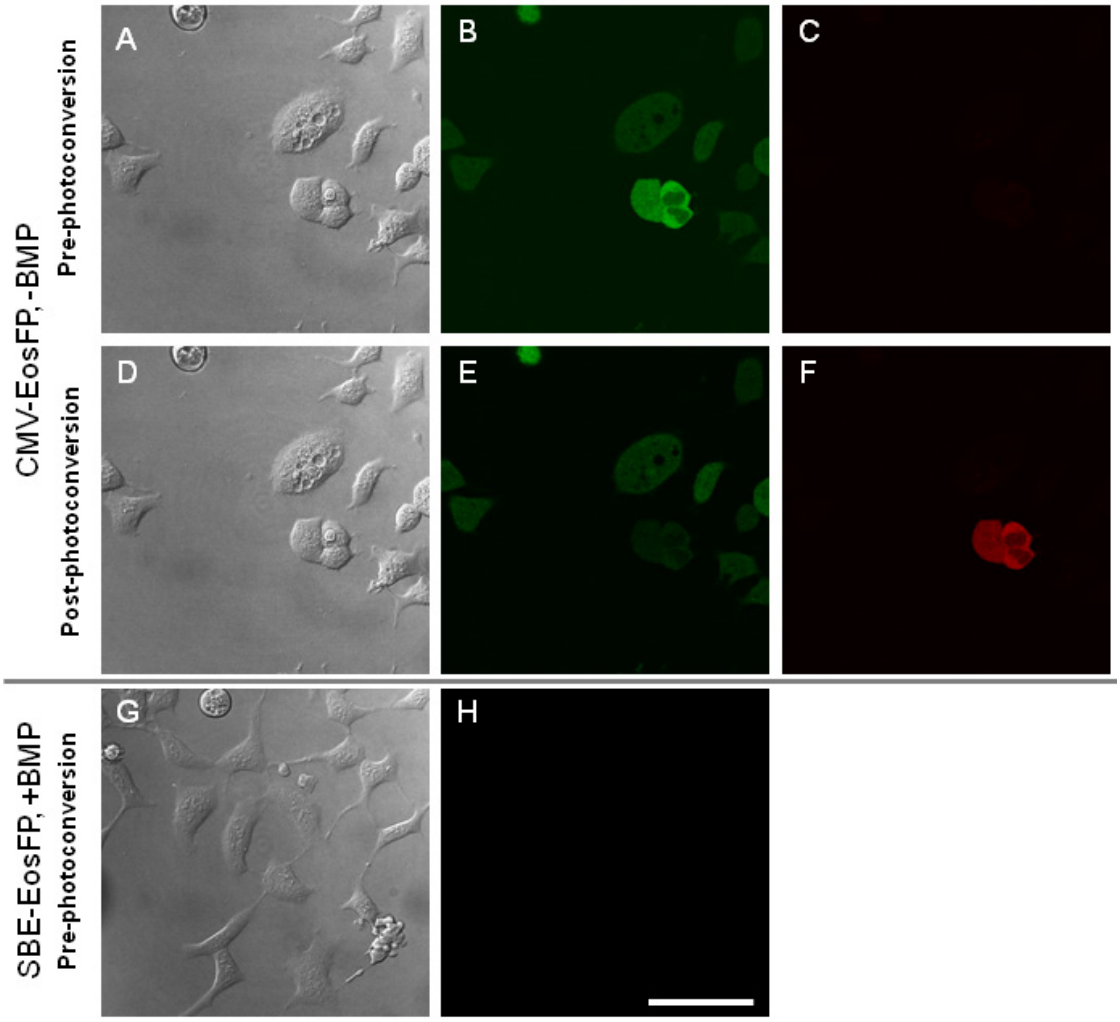

Figure 13: Test of induction of SBE-EosFP in stable cell lines. (A-F) EosFP under CMV promoter fluorescence constantly green and underwent photo-conversion. (G, H) No fluorescence of EosFP was observed with SBE construct. Bar 75 µm.

As shown in Figure 13, green fluorescence was detected in most cells bearing CMV-EosFP, in which EosFP was constitutively expressed (B, E). This means that the procedure for establishing stable cell line was successful. The green fluorescence of EosFP could be photo-converted into red (F). Unfortunately, we failed to detect any green fluorescent cells in the stable cell line bearing SBE-EosFP constructs (H).

3.1.5 Discussion

In this section of study, we screened three available photo-switchable fluorescent proteins and found that EosFP was the best one under our experimental conditions. Mainly due to its fast maturation at 28°C, EosFP represented the best psFP as a reporter in zebrafish system. The UV-induced photo-conversion was also achieved in zebrafish under our home-made SPIM setup.

Nonetheless, the reporter-driving cis-element, namely SBE, did not function to response in cultured cell lines. We argued that such lack of fluorescence might very likely due to the expression level upon stimulation. Although SBE was used to assay the subjection of target cells to extracellular TGF-/BMP stimuli, most of the studies were done using luciferase as a reporter (enzyme catalyzed reaction) and the signal was detected from population of cell in presence of over-expressed Smad proteins (Jonk et al, 1998). Therefore, signals detected in previous work on SBE-luc were the result of amplification of at least 2 different levels due to the detection reaction itself and a large amount of cells being analyzed. However, the FP reporter was confined in individual cells in our system.

Another possibility could be that the induction with SBE was not efficient enough. Shortly after SBE, a BMP-responsive element was identified, which contain two regions of mouse Id1 promoters and was proven to be appropriate for BMP responsiveness (Korchynskyi & ten Dijke, 2002). Such element has been applied in a number of studies to detect BMP/Smad signaling *in vivo*. By the time of this thesis, transgenic animals have been described in different model systems including zebrafish (Collery & Link, 2011; Laux et al, 2011). Because the SBE construct was not promising and such a BRE construct was not available at that time, we sought to investigate the signaling by alternative approach.

3.2 Spatiotemporal visualization of Smads activation *in vivo*

Smad proteins are central to BMP signaling as intracellular transmitters. In the canonical pathway, R-Smads get phosphorylated by membrane-anchored receptor upon ligand

activation, form complex with Smad4, enter nucleus and perform their transcription factor functions (Massague et al, 2005). To date, three R-Smads have been identified that mediate BMP signaling in mammalian cells (BR-Smads), namely Smad1, Smad5 and Smad8 (known also as Smad9). Although their highly conserved amino acid sequences implies possible functional interchangeability, differences amongst these three intracellular signal transmitters has not been fully characterized (Miyazono et al, 2010). Therefore, it is an alternative of interest to investigate the spatiotemporal activation of individual Smad activation in terms of their possible distinct transmitting activity upon BMP stimulation.

As Smads have to undergo cytoplasm-nucleus translocation to act as effectors, we thus would like to take advantage of fluorescence microscopy and track on the cyto-nucleo translocation of R-Smads in different embryonic area at real time. When the cell membrane and nucleus are marked as summarized in the Figure 14, the Smad neucleo-translocation can be derived from nucleus-to-cytosol ratio of GFP-intensity.

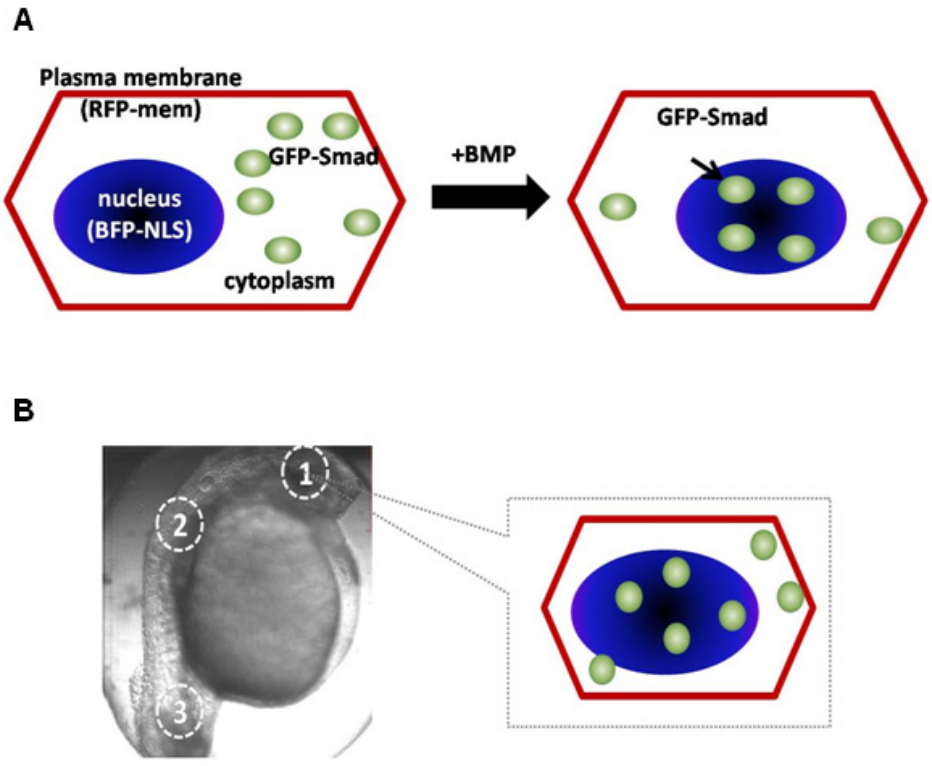

Figure 14: Schematic diagram for Smad nucleotranslocation determination. (A) Plasma

membrane and nucleus are red and blue labeled as reference and Smad protein is labeled as green. (B) With aid of cellular compartment labeling, sub-cellular localization of Smad protein is readily calculated from green fluorescence at region of interest at a given development stage of zebrafish embryo.

We would like to investigate this *in vivo* using zebrafish as model system. To do so, we take advantage of Tol2 transposon mediated gene-delivery system. As shown in Figure 15, this system consists of two components, namely a messager RNA encoding Tol2 transposase and a plasmid DNA with gene of interest flanked between 2 Tol2 *cis*-elements. Upon injection into the fertilized egg at 1-cell stage, the newly and transiently synthesized transposase helps the integration of the transposon construct onto genomic DNA in a "cut-and-paste" manner. The resulting founder fish is raised till adult and eventually cross with wild type fish to produce transgenic fish lines.

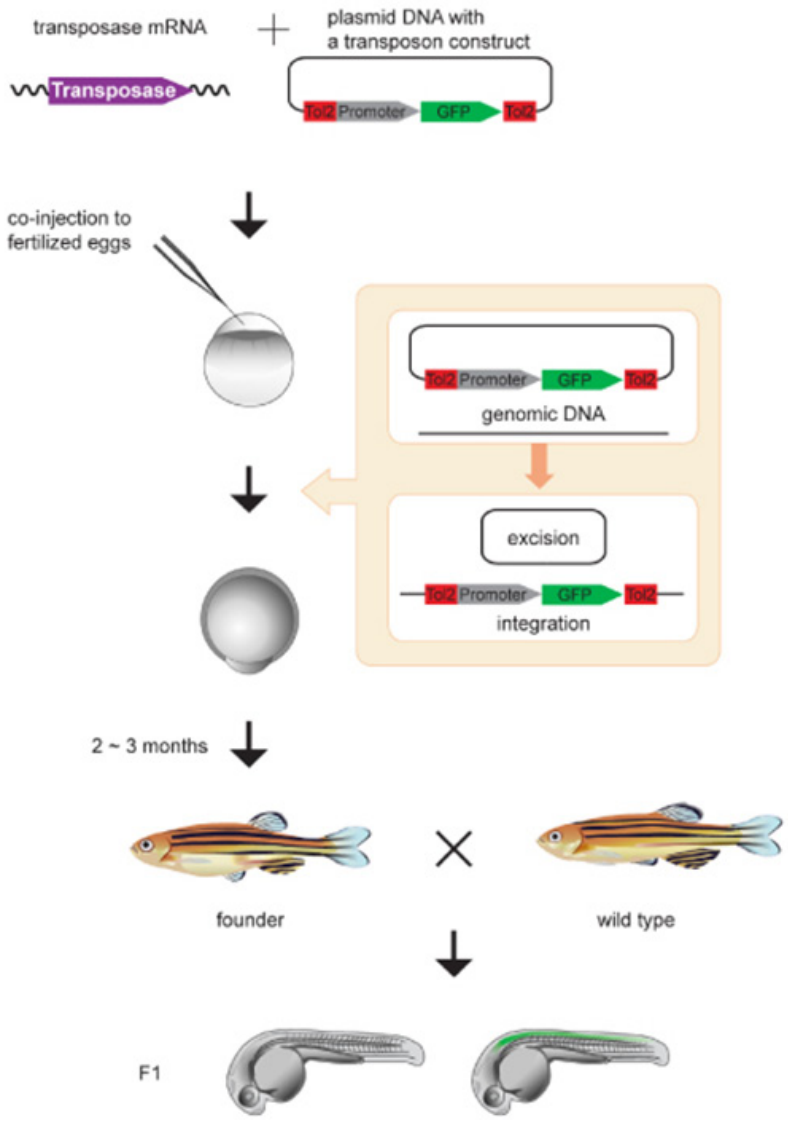

Figure 15: Schematic diagram for Tol2-transposon mediated trangenesis in zebrafish. The synthetic transposase mRNA and a transposon donor plasmid containing a Tol2 construct with a promoter and the gene encoding green fluorescent protein (GFP) are co-injected into zebrafish fertilized eggs. The Tol2 construct is excised from the donor plasmid and integrated into the genome. Tol2 insertions created in germ cells are transmitted to the F1 generation. Germ cells of the injected fish are mosaic, and, by crossing the injected fish (founder) with wild-type fish, nontransgenic fish and transgenic fish heterozygous for the Tol2insertion are obtained. In this figure, the promoter is tentatively defined as a spinal cord specific enhancer/promoter and the spinal cord of the embryo is depicted in green. Diagram is from (Kawakami, 2007)

3.2.1 Isolation of zebrafish full-length Smad cDNAs

Total RNAs were extracted from mixed zebrafish embryos from different development stages ranging from 1-cell stage to 24 hours post fertilization. Using this RNA as template and oligo-dT as primers, full-length cDNAs were reverse transcribed and used to amplify zebrafish Smad (zSmad) genes with gene-specific primer pairs.

We successfully isolated full-length coding sequences for zSmad1, zSmad4, zSmad5 and zSmad8. As shown in Figure 16, they are very similar to each other in the amino acid sequence due to homology.

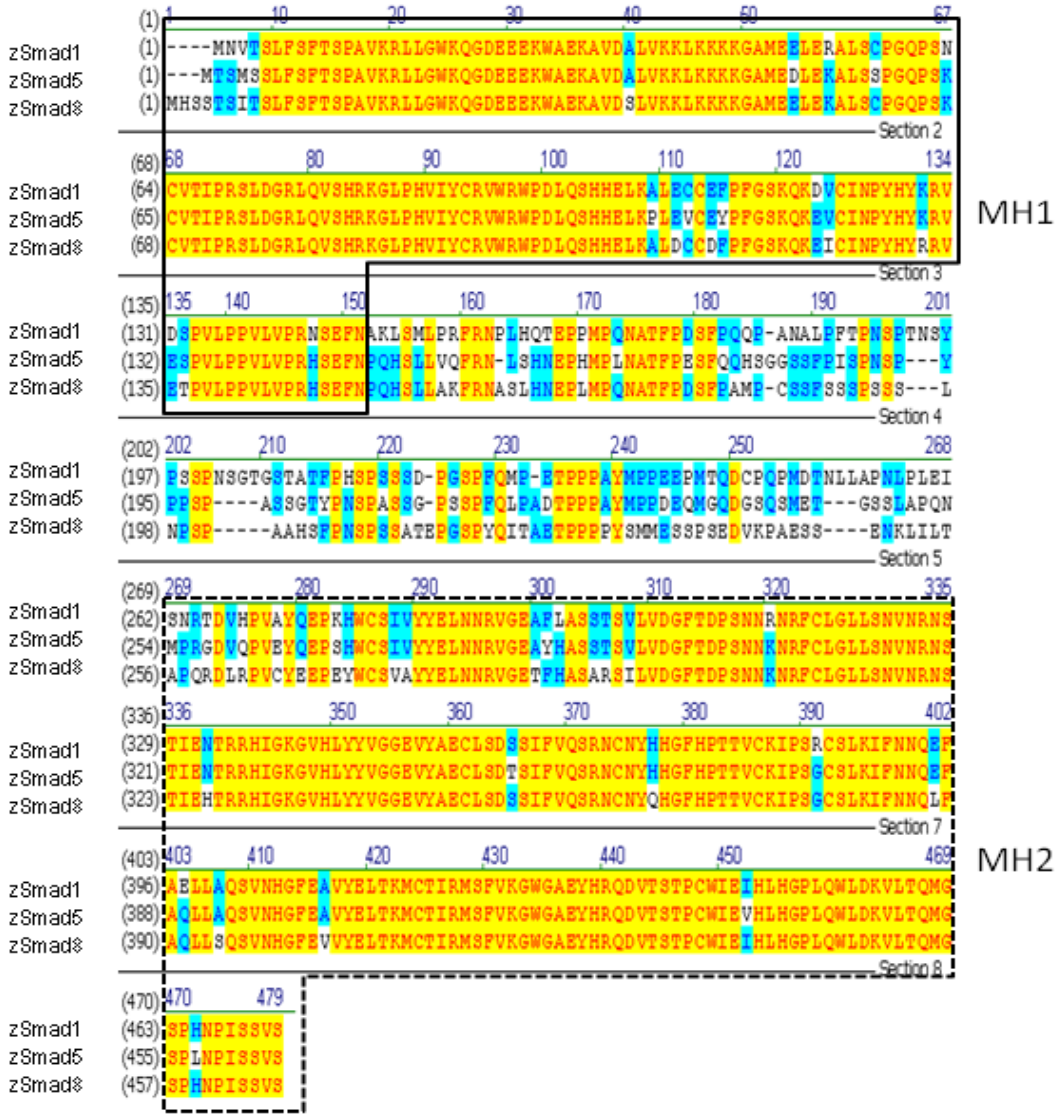

Figure 16: Alignment of isolated zebrafish Smad genes. Smad1, Smad5 and Smad8 coding sequences were isolated from zebrafish (TÜ). The translated coding sequences were

aligned by VectorNTI software (Invitrogen). Mad homolog (MH) domains were highlighted: MH1 in solid line while MH2 in dotted line.

3.2.2 Construction of GFP-Smad fusions and their sub-cellular localization *in vitro*

To help study the sub-cellular localization of the Smad proteins, we create a helper parental plasmid, which allows simultaneous expression of membrane marker, nucleus marker and Smad-fusions with distinct FPs. The reason for constructing the helper plasmids is to reduce the transgenic zebrafish lines and the time for experiment preparation. If we create transgenic fish lines for Smad-fusion and for cellular compartment labeling, we will have to cross them so as to have all the elements together necessary for analysis, meaning at least 2 to 3 generations will be needed to have the fish. Instead, one line for each Smad-fusion and cellular compartment labeling can be constructed together.

This is achieved by connecting three open reading frames (ORFs) with a so-called “2A” peptide as shown in Figure 17B (Szymczak & Vignali, 2005; Szymczak et al, 2004; Toramoto et al, 2004). This will lead to one messager RNA after transcription (Figure 17A). Because the ribosome cannot make peptide bond between glycine and proline which is intentionally added in the “2A” sequence between the ORFs, it will “skip” the glycine-proline and continue to translate the mRNA to the end. As a consequence, three proteins will be synthesized.

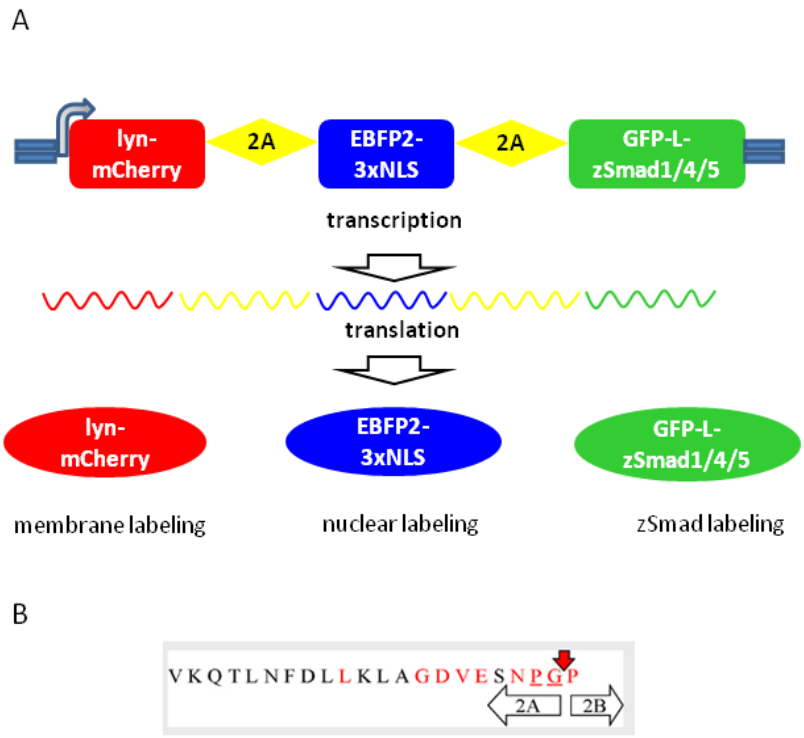

Figure 17: Multi-cistron construct based on "2A" enables co-expression of multiple genes simultaneously. (A) One single plasmid encoding three cistrons flanked by "2A" peptide is transcribed to one mRNA, which after translation results in three proteins. (B) Consensus sequence of "2A" peptide, from (Toramoto et al, 2004).

We then cloned the isolated zSmad into the expression plasmid under *Xenopus* elongation factor 1α promoter ($P_{EF1\alpha}$) (Johnson & Krieg, 1994) to check whether we were able to study the subcellular localization of Smad proteins inside the cells (Table 5).

Table 5 Multiple cistronic constructs based on "2A" for zebrafish Smads

Plasmid	Property	Purpose
pcDNA3.1(+)	Eukaryotic expression with CMV promoter	Over-expression in mammalian cell lines, Invitrogen
p2A	pcDNA3.1(+) with CMV replaced by *Xenopus* EF1α promoter and 2A based multiple cloning sites	Over-expression in mammalian cell line , for multiple genes co-expression
p2A-red-mem-blue-nuc	hLynmCherry-2A-EBFP2-3xNLS	Co-expression of membrane-target mCherry and nucleus-targeted EBFP2
p2A-red-mem-blue-nuc-green zSmad1	hLynmCherry-2A-EBFP2-3xNLS-meGFP-zSmad1	Co-expression of membrane-target mCherry, nucleus-targeted EBFP2 and meGFP tagged zebrafish Smad1
p2A-red-mem-blue-nuc-green zSmad4	hLynmCherry-2A-EBFP2-3xNLS-meGFP-zSmad4	Co-expression of membrane-target mCherry, nucleus-targeted EBFP2 and meGFP tagged zebrafish Smad4
p2A-red-mem-blue-nuc-green zSmad5	hLynmCherry-2A-EBFP2-3xNLS-meGFP-zSmad5	Co-expression of membrane-target mCherry, nucleus-targeted EBFP2 and meGFP tagged zebrafish Smad5

As shown in Figure 18, both cell membrane and nucleus were successfully labeled as red and blue with fluorescent proteins mCherry and EBFP2 (A, B, D, E, G, H). zSmads were detected by green fluorescence from GFP. zSmad4 and zSmad5 were predominantly detected in cytoplasm while zSmad1 was surprisingly detected in nucleus (C, F, I).

Such an observation was interesting because under prevailing assumption, only small proportion of Smad proteins will undergo nucleo-translocation under activation. We argued that the zebrafish Smad1 might behave differently in mammalian cell lines. We then further analyze their localization and activation in zebrafish.

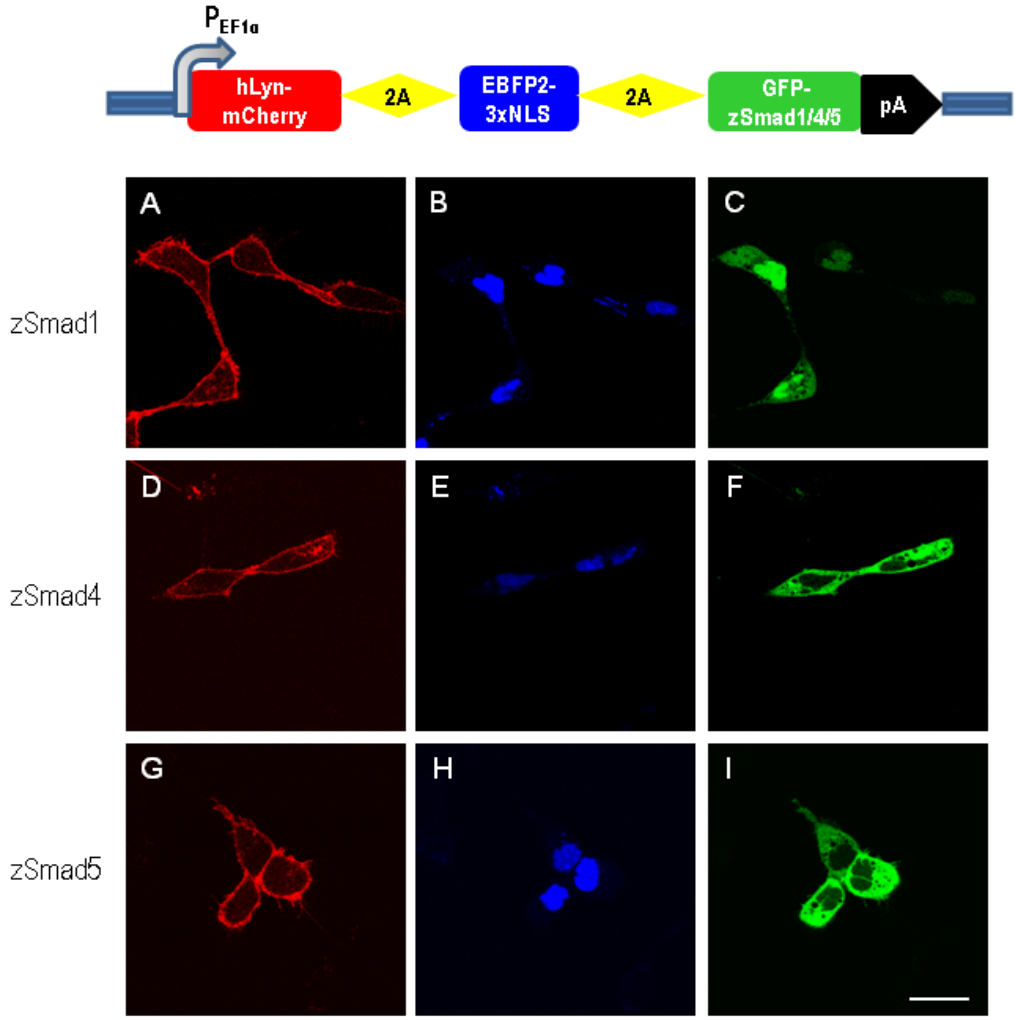

Figure 18: Test of "2A" constructs and sub-cellular zebrafish Smad proteins in cells. Constructs listed in Table 5 were used to transfect HEK293 cells and sub-cellular localization of zSmads was observed with confocal microscopy. Bar 50 µm.

3.2.3 Generation of appropriate delivery plasmid for transgenic zebrafish

We intended to generate transgenic zebrafish with the Tol2 transposon gene-delivery system to study the Smad activation *in vivo*. The flowchart was described in previous section (Figure 15). Nevertheless, we were in need of an appropriate vector to do so.

As shown in Figure 19A, the miniTol vector bears the essential Tol2 *cis*-elements, the 5'- and 3'-untranslated regions (5'-and 3'-UTRs), which are able to mediate transposition in presence of transposase activity (Balciunas et al, 2006). However, to allow expression of

a exogenouse gene, more elements are required, such as an appropriate promoter for expression and a polyA signal for stabilization. We compared the performance between the Human cytomegalovirus promoter (P_{CMV}) and the *Xenopus* Elongation Factor 1α ($P_{EF1\alpha}$) (Johnson & Krieg, 1994). As depicted in Figure 19B, the exogenous CMV promoter led to considerate expression, but not even (left). The expression driven by EF1α promoter was characterized by both even and adequate (right).

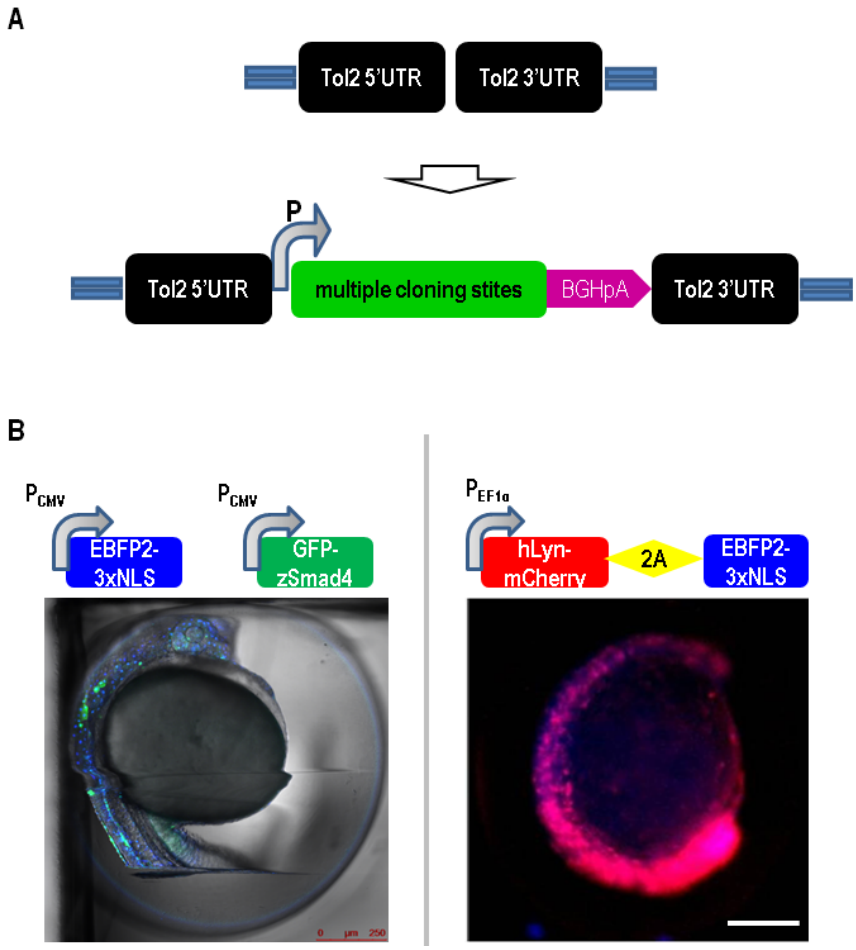

Figure 19: Construction of parental plasmid for transgenesis of zebrafish. BMP-directedpminiTol2 was modified to add two additional elements, a functional promoter and a BGH polyA signal (A). Expression pattern with CMV promoter and *Xenopus* EF1α were compared (B). Bar 250 µm.

We therefore constructed the following plasmids under EF1α promoter, as listed in Table 6.

Table 6 Constructs made to create transgenic zebrafish

Plasmid	Property	Purpose, Source
pminiTol2/MCS	Tol2 transposon vector	Transposition in vertebrates including zebrafish, Lab Manfred Schartl, (Balciunas et al, 2006)
pT3T/MCS	Tol2 transpase	Template for Tol2 transposase production, Lab Manfred Schartl, (Balciunas et al, 2006)
pTol2	pminiTol2 with EF1α promoter and BGH	Over-expression in mammalian cell line , for multiple genes co-expression
pTol2/2A-red-mem-blue-nuc	hLynmCherry-2A-EBFP2-3xNLS	Co-expression of membrane-target mCherry and nucleus-targeted EBFP2
pTol2/2A-red-mem-blue-nuc-green zSmad1	hLynmCherry-2A-EBFP2-3xNLS-meGFP-zSmad1	Co-expression of membrane-target mCherry, nucleus-targeted EBFP2 and meGFP tagged zebrafish Smad1
pTol2/2A-red-mem-blue-nuc-green zSmad4	hLynmCherry-2A-EBFP2-3xNLS-meGFP-zSmad4	Co-expression of membrane-target mCherry, nucleus-targeted EBFP2 and meGFP tagged zebrafish Smad4
pTol2/2A-red-mem-blue-nuc-green zSmad5	hLynmCherry-2A-EBFP2-3xNLS-meGFP-zSmad5	Co-expression of membrane-target mCherry, nucleus-targeted EBFP2 and meGFP tagged zebrafish Smad5
pTol2/green zSmad1	meGFP-zSmad1	Over-expression of meGFP tagged zebrafish Smad1
pTol2/green zSmad4	meGFP-zSmad4	Over-expression of meGFP tagged zebrafish Smad4
pTol2/green zSmad5	meGFP-zSmad5	Over-expression of meGFP tagged zebrafish Smad5

3.2.4 Generation of transgenic zebrafish lines with over-expressed zSmad fusions

The trial to create transgenic fish with three products failed as shown in Figure 20A. The reason was less understood. Because Tol2 transposon system has been characterized to be

able to deliver up to 11 kb cargo sequence without noticeable loss of transposition efficiency (Balciunas et al, 2006; Urasaki et al, 2006) and our largest construct was less than 4 kb, we argued the reason why we did not observe the reporter in micro-injected F0 fish might be due to the failure of transcription. This is beyong our scope to further address such causality in this study. Meanwhile, expression of 2 cellular markers was detected in trail with corresponding plasmid (Figure 20B, left). Hence we planned to create transgenic fish lines, one line bearing cellular markers and others bearing individual zSmad fusions. By crossing the offspring, we would get all the three products within one line to be able to analyze each zSmad activation (Figure 20B).

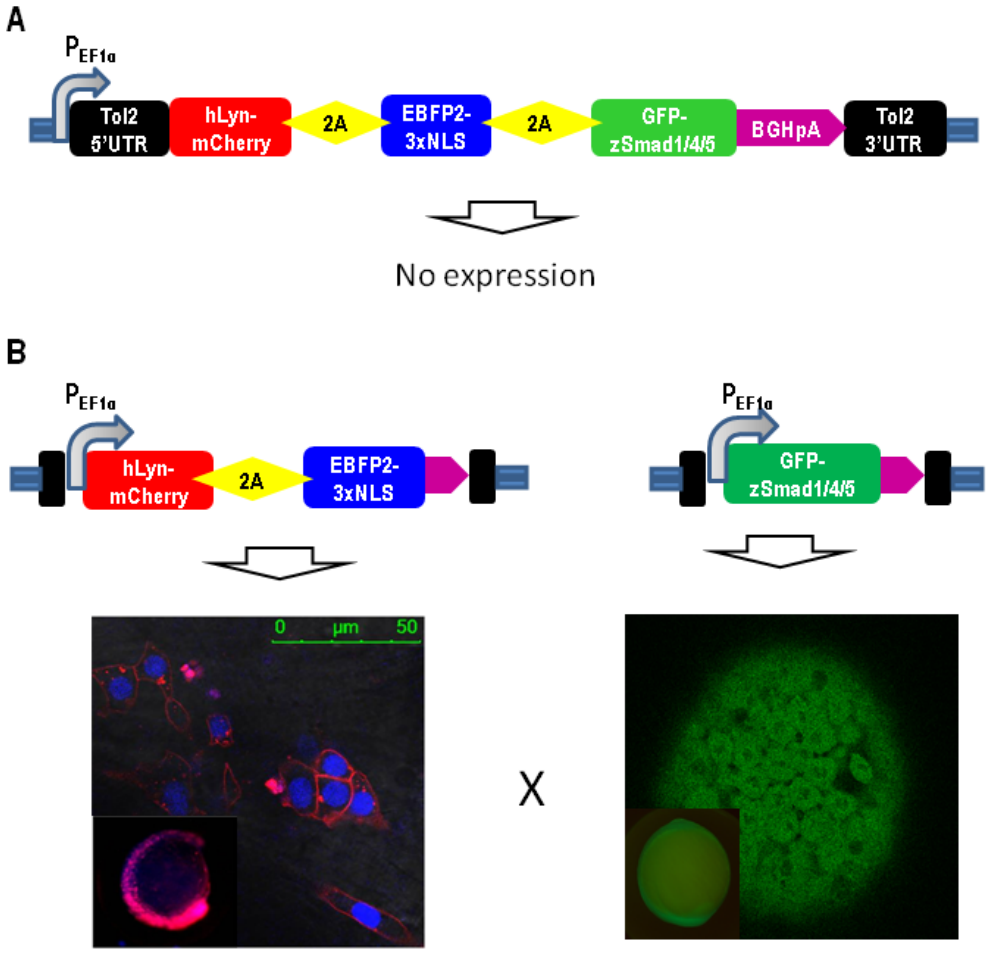

Figure 20: Generation of transgenic zebrafish with "2A"-based Tol2 constructs. (A) Constructs for three-cistronic expression were not functional. (B) Nevertheless, construct encoding cellular compartments as well as constructs for meGFP-tagged individual zSmads were functional. Bar 250 µm.

With these validated constructs, we micro-injected wild-type zebrafish embryos at 1-4 cell stage and created transgenic zebrafish lines for analysis. Table 7 lists the transgenic fish lines created via collaboration in Lab Soojin Ryu by Boris Knerr at the Max-Plank-Institute for medical research Heidelberg.

Table 7 Transgenic zebrafish lines

Fish line	generation	NB
Tg(Elf1α:msfGFP-zfSmad1)	F0	~50 Juveniles
Tg(Elf1α:msfGFP-zfSmad4)	F0	~50 Juveniles
Tg(Elf1α: lynCherry-2A-H_2B-BFP2)	F0	~50 Adults
Tg(Elf1α:msfGFP-zfSmad5)Fd1	F1	~12 Adults
Tg(Elf1α:msfGFP-zfSmad5)Fd2	F1	~10 Adults
Tg(Elf1α:msfGFP-zfSmad5)Fd3	F1	~7 Adults
Tg(Elf1α: lynCherry-2A-BFP2-3xnls)Fd2	F1	~8 Adults
Tg(Elf1α: lynCherry-2A-BFP2-3xnls)Fd4	F1	~4 Adults
Tg(Elf1α: lynCherry-2A-BFP2-3xnls)Fd5	F1	~3 Adults
Tg(Elf1α:msfGFP-zfSmad5)Fd1	F2	~15 Juveniles
Tg(Elf1a:msfGFP-zfSmad5)Fd1 x Tg(Elf1a:lynCherry-2A-BFP2-3xnls)Fd2	F2	~20 Juveniles
Tg(Elf1a:lynCherry-2A-BFP2-3xnls)Fd4	F2	~20 Juveniles

3.2.5 Static analysis of the Smad activation during zebrafish development with immune-staining

Because the C-terminal SSVS sequence is conserved in all R-Smads in zebrafish as well as in mammalians without exception, and receptor-mediated Phosphorylation is essential for Smad activation, it has been applied to determine the activation of Smad frequently using an anti-phospho-Smad1/5/8 antibody (α-pSmad) in immuno-blotting as well as immune-staining analyses (Tucker et al, 2008).

We, therefore, performed the immune-staining of zebrafish embryos against pSmad. In agreement with previous studies, the onset of BMP signaling, as indicated by the p-Smad staining, was observed about 6 hours post fertilization (hpf) at the shield stage (Figure 21A, B, C).

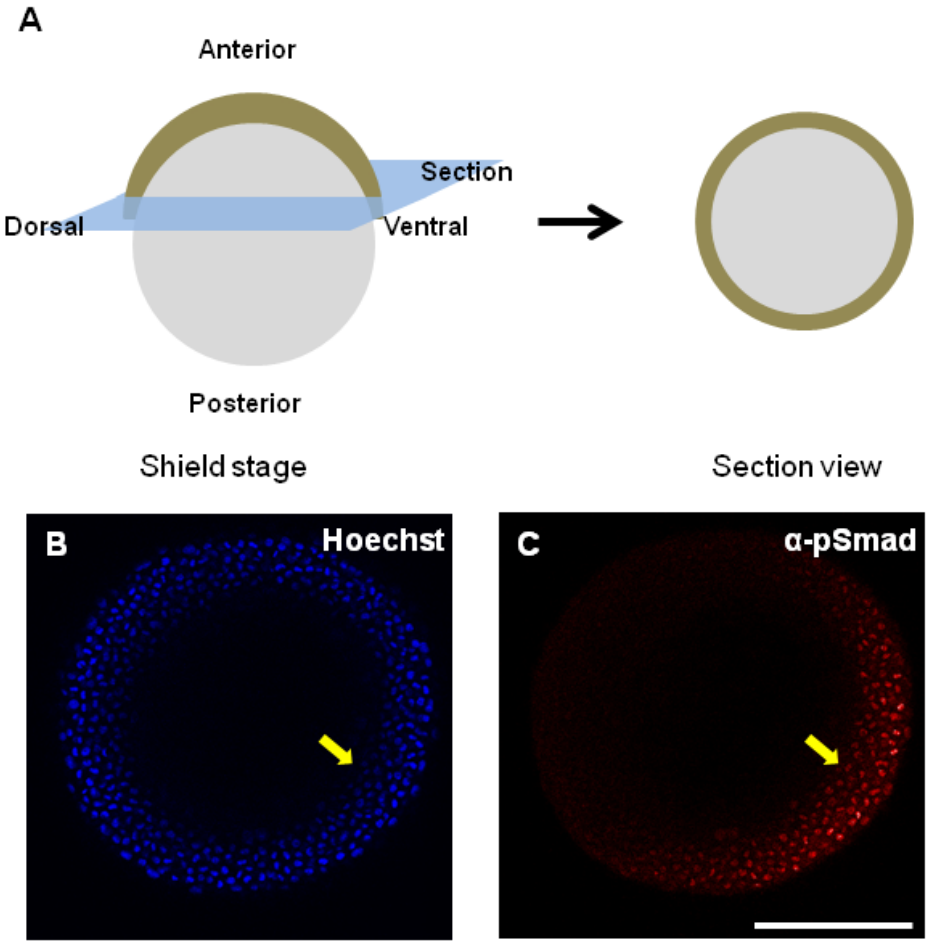

Figure 21: Immmuno-staining of phospho-Smad in developing zebrafish embryos at shield stage

(~6 hpf). (A) Schematic drawing of a shield stage zebrafish embryo and its section view. (B, C) stained embryo with Hoechst (B) or with α-pSmad (C) were imaged under confocal microscope and representative section was shown. Yellow arrows indicate the future ventral side. Bar 250 µm.

The signaling propagated further through bud stage and somite (ca. 12 hpf, Figure 22A, B and C). Notably, asymmetrical distribution of such signaling was visualized. The p-Smad was only found at one side of the embryo (the future ventral side) at the shield stage and at tail-bud when it reached somite stage as indicated with yellow arrows (Figure 21 and 22).

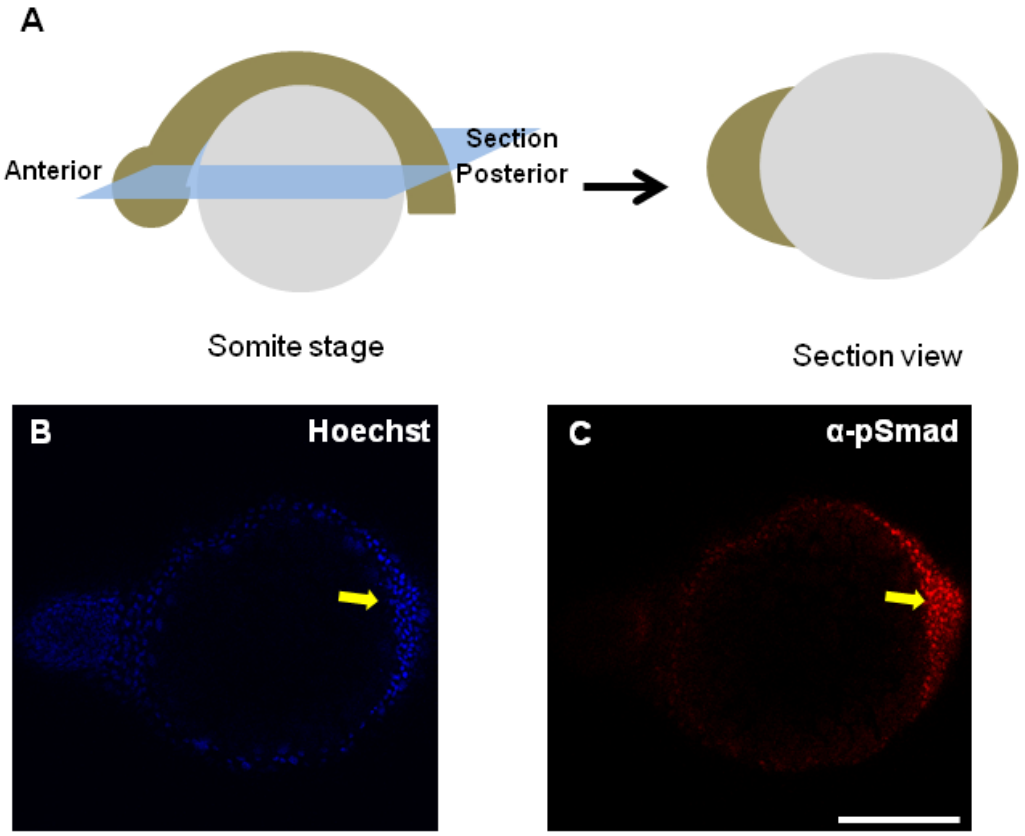

Figure 22: Immmuno-staining of phospho-Smad in developing zebrafish embryos at somite stage (~12 hpf). (A) Schematic drawing of a somite stage zebrafish embryo and its section view. (B, C) stained embryo with Hoechst (B) or with α-pSmad (C) were imaged under confocal microscope and representative section was shown. Yellow arrows indicate tail-bud. Bar 250 µm.

3.2.6 Dynamic analysis of the Smad nucleo-translocation during zebrafish development with over-expressed Smad

Since the p-Smad staining was obvious at these two stages, we would like to investigate the difference of individual R-zSmad activation at these two stages.

Transgenic zebrafish over-expressing GFP-tagged zSmad5 was analyzed by confocal microscopy. Fish embryo was embedded in 1% agarose at viable temperature for fish to survive. We observed accumulation of GFP signal in transgenic Smad5 fish embryo at shield stage, indicating nucleo-translocation of zSmad5 (Figure 23). The region where Smad5 is predominantly neucleus-localized was also asymmetric similar to the observation with p-Smad antibody staining (Figure 21C).

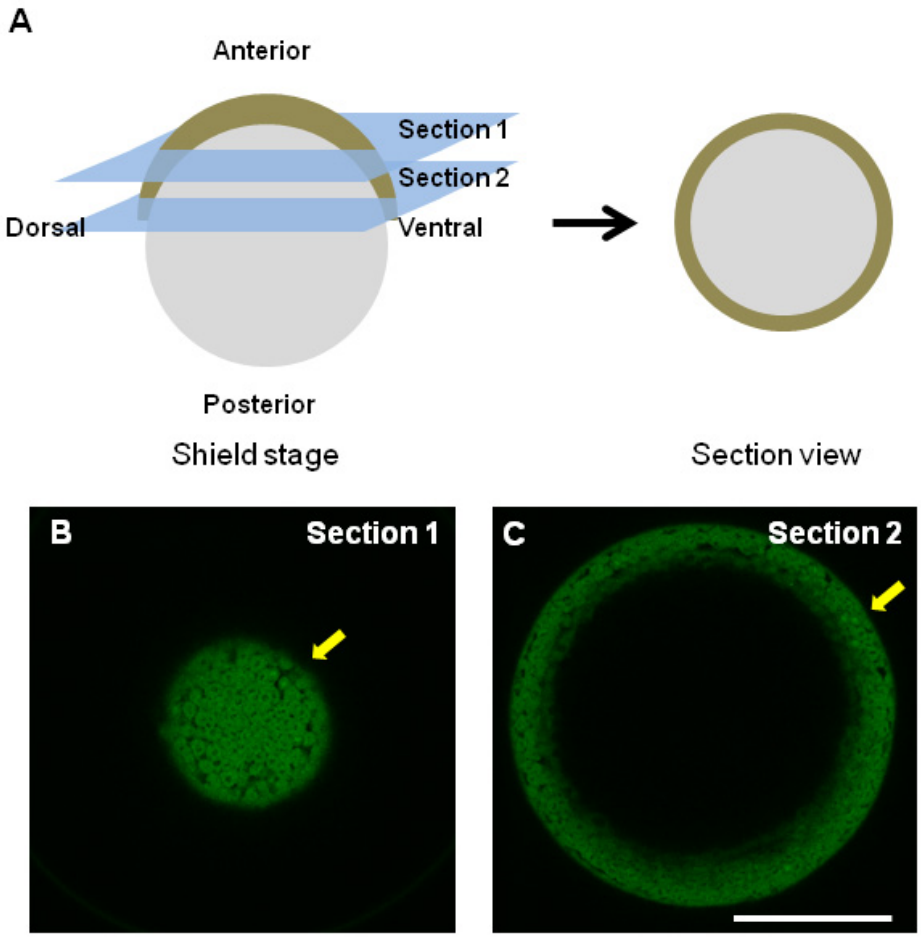

Figure 23: Real-time imaging of GFP-tagged zSmad5 in developing transgenic zebrafish embryos at shield stage (~6 hpf). (A) Schematic drawing of a shield stage zebrafish embryo and its section view. (B, C) live embryo were imaged under confocal microscope

and representative images at different z-position were shown. Yellow arrows indicate nuclear accumulation of zSmad5. Bar 250 µm.

We also analyzed the cellular localization of zSmad1 in zebrafish. Since transgenic zebrafish line for zSmad1 was not available yet, we performed transient over-expression. Figure 24 summarized the observation with Smad1. In contrast to zSmad5, Smad1 was observed to be generally nucleus-localized. This is in agreement with the observation in cell line (Figure 18).

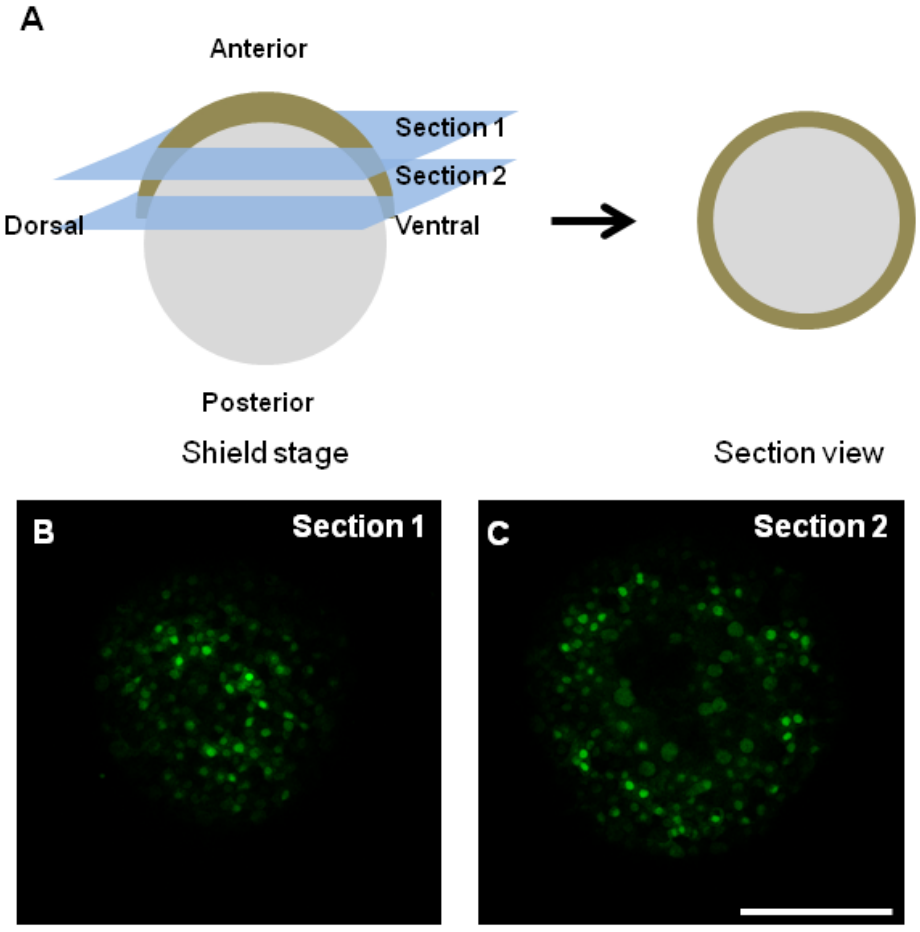

Figure 24: Real-time imaging of GFP-tagged zSmad1 in developing zebrafish embryos at shield stage (~6 hpf). (A) Schematic drawing of a shield stage zebrafish embryo and its section view. (B, C) live embryo were imaged under confocal microscope and representative images at different z-position were shown. Bar 250 µm.

3.2.7 Correlation of Smad localization to Phosphorylation

To validate the correlation of nucleus-accumulation to phosphorylation, we repeated the imaging with immuno-staining together. As shown in Figure 25, cells with nucleus-accumulated zSmad5 were observed, which overlapped the phosphor-Smad staining pattern (Figure 25A, B, C; yellow arrows). This observation clearly demonstrates that zSmad5 is phosphorylated and under goes nucleo-translocation at onset of gastrulation (shield) of zebrafish development.

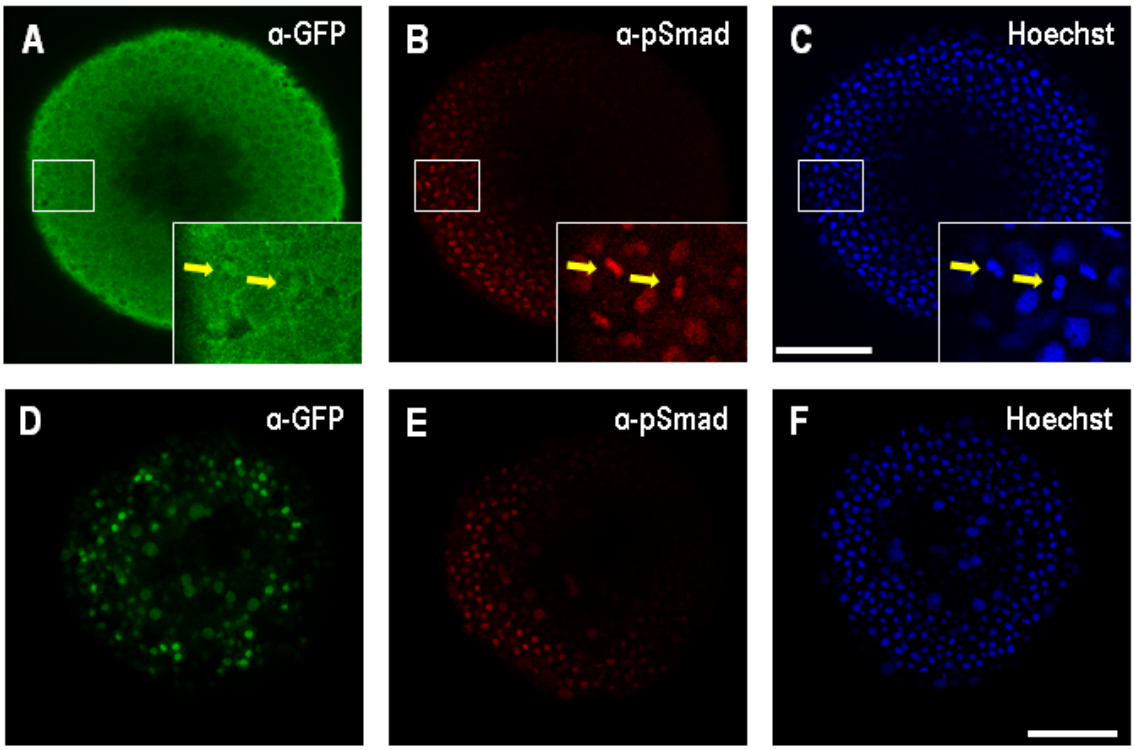

Figure 25: Correlation of Smad nucleus-accumulation to phosphorylation. Zebrafish embryos at shield stage (~6 hpf) were fixed, immunostained against GFP (α-GFP) and phosphor-Smad1/5/8 (α-pSmad) and imaged under confocal microscope. (A, B, C) Representative sections of immuno-staining were shown for transgenic GFP-zSmad5, where yellow arrows indicate noticeable nucleo-translocation of zSmad5. (D, E, F) Representative sections of immuno-staining were shown for transient GFP-zSmad1 zebrafish embryo. Bar 250 µm.

However, the zebrafish Smad1 was observed to be prominently localized in the nucleus

irrespective of the status of phosphorylation (Figure 25D, E, F). Such an observation was in agreement with the results acquired in the cell line studies (Figure 18).

3.2.8 Quantification of zSmad nucleo-translocation during zebrafish development with real-time SPIM imaging and Volocity software

Although we have made several transgenic zebrafish lines, we have unfortunately not acquired enough stable adult lines for cross to make three color fishes for analysis (Table 7). However, we perform transient injection of *in vitro* synthesized mRNA encoding same products to investigate the Smad motility in zebrafish.

The algorithms about how we quantify the nucleo-translocation of zSmad is explained in Figure 26. Ideally, the cross between transgenic zebrafish lines will give rise to fish lines where cellular markers and one of zSmad are present (Figure 26A). Alternatively, all three essential labeling can also be brought together into one zebrafish embryo by simultaneous co-injection. With the nucleus labeling, the amount of nucleus-localized zSmad is readily calculable. To be able to calculate the cytosolic zSmad quantity, we have two options. In a so-called “2-label calculation”, cytosol is calculated by subtracting the nucleus fraction from cellular volume defined by membrane labeling (Figure 26B, left). The so-called “1-label calculation” takes advantage of the Volocity software’s function to enlarge the nucleus to create a partial cytosol next to the nucleus (Figure 26B, right).

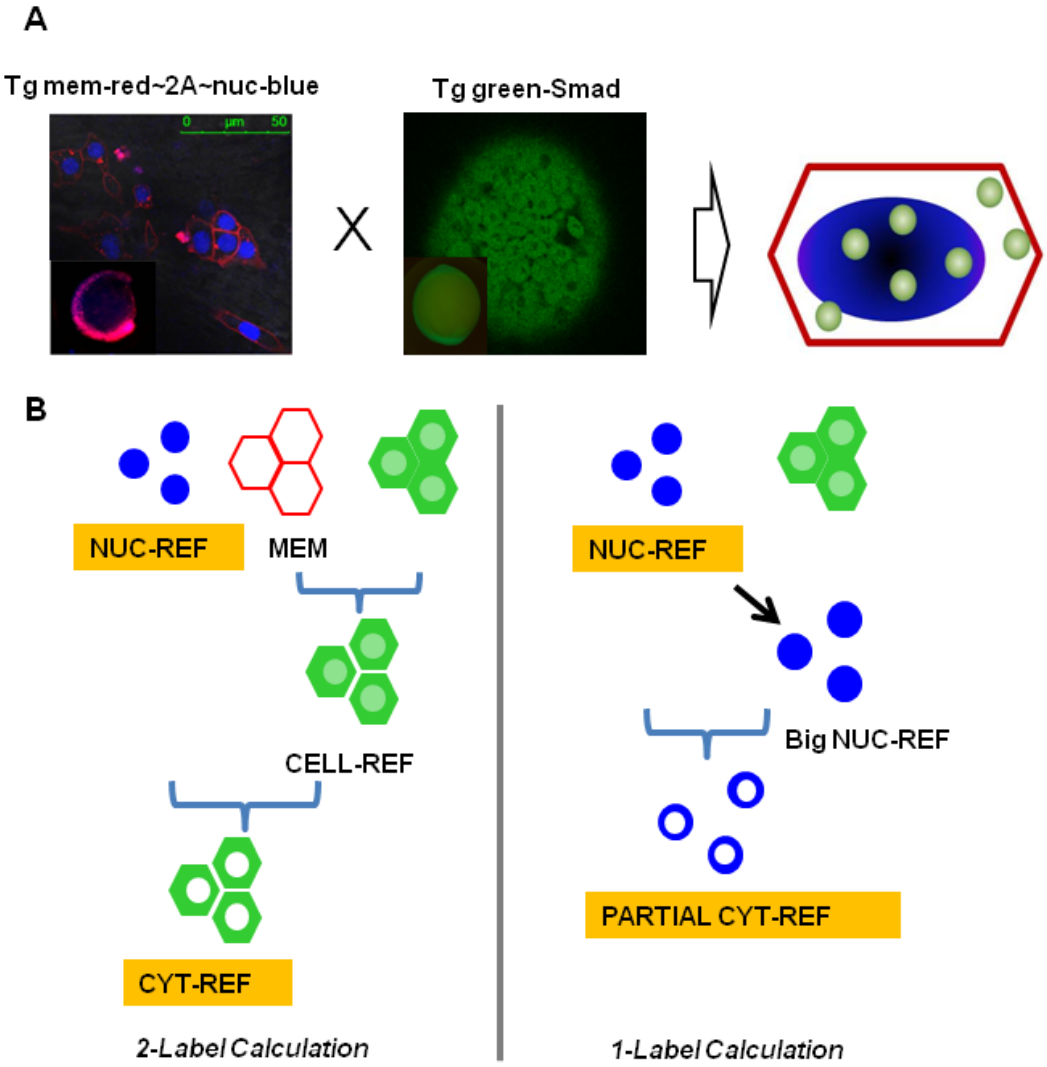

Figure 26: Schematic diagram for quantification of zSmad nucleo-translocation. (A) Generation of zebrafish by crossing transgenic lines. (B) Calculation of nucleo-translocation of zSmad via "2-label Calculation" (left) or via "1-label Calculation" (right).

We performed micro-injection of mixed *in vitro* transcribed mRNAs and imaged the FP-labeled zSmad1 and zSmad5 simultaneously with SPIM. As depicted in Figure 27, the nucleus was labeled as blue (hH_2B-EBFP2); zSmad1 and zSmad5 were labeled as green (mGFP-zSmad1) and red (mCherry-zSmad5) respectively.

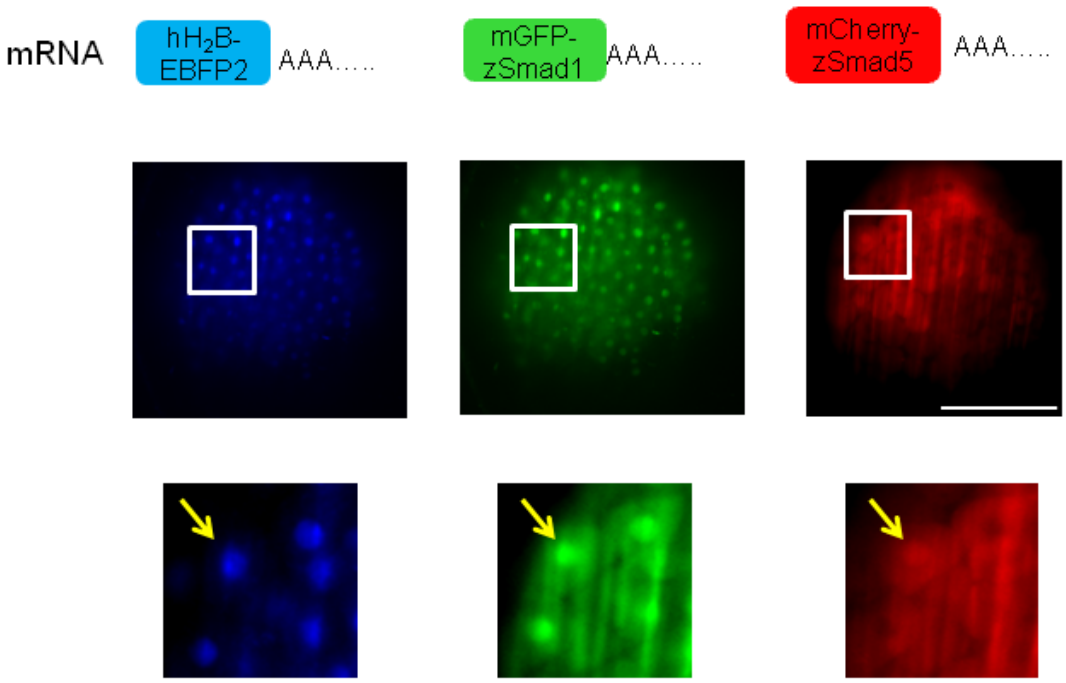

Figure 27: Quantification of zSmad nucleo-translocation. *In vitro* transcribed mRNAs were micro-injected into zebrafish embryo at 1-4 cell-stage. ~6 hpf, positive embryos were sorted for fluorescence and imaged with SPIM. Images were processed with ImageJ and regions of interest (white square) were enlarged. A representative cell was highlighted with a yellow arrow. Bar 100 µm.

We analyzed the sub-cellular localization of zSmad1 and zSmad5 with Volocity software. Since only one nucleus label was available, we followed "1-label calculation". Table 8 summarizes the results of the analysis. In a few cells with predominant nucleus-localized zSmad5, we had a nucleus-to-cytosol ratio (Ratio nuc/cyt) about 1.2. In contrast, we had a Ratio nuc/cyt of about 0.8 in the large number of other cells with predominant cytosolic zSmad5 localization. Such a differentiated Ratio was not observed in the calculation of zSmad1, which had a nuc/cyt ratio about 2.1 in next to all cells analyzed.

Table 8 Analysis on sub-cellular localization of zebrafish Smad1 and Smad5 during gastrulation

Smad	Positive cells (nucleo-translocation observed)	Negative cells (nucleo-translocation observed)	BMP Signal Detection
zSmad5	Ratio nuc/cyt=1.20±0.10 (n≈20 cells)	Ratio nuc/cyt=0.83±0.10 (n>200 cells)	applicable
zSmad1	Ratio nuc/cyt=2.10±0.10(n>200 cells)		not applicable

3.2.9 Discussion

In this section of study, we isolated Smad genes from zebrafish, generated their fusions to fluorescent proteins. We analyzed the sub-cellular localization of zSmads both in cell lines as well as in zebrafish embryo. Although zebrafish Smad1, Smad5 and Smad8 share significant conserved sequences, they are localized differently in mammalian cells. zSmad5 and zSmad8 were observed to be predominantly cytosol-localized while zSmad1 in nucleus.

We constructed Tol2-transposon plasmids bearing FP-zSmad fusions as well as cell-compartment labeling. Transgenic zebrafish lines were generated with these constructs. We analyzed the sub-cellular localization of zSmads in live zebrafish embryos with high resolution microscopy. The zebrafish Smad5 protein was observed to be nucleus-localized in a number of cells which were also positive with p-Smad immuno-staining at shield stage. This observation is in agreement with the previous results demonstrating the BMP's signaling at onset of gastrulation. It is therefore very likely that zSmad5 is regulated by the endogenous BMP signal at the observed development stage.

We had unexpected results with zSmad1, however. We observed predominant nucleus localization for zSmad1 not only in cell line, but also in zebrafish. Thus, the cellular environment seemed unlikely to affect the sub-cellular localization of zSmad1. Moreover, we did not observe an increased nucleus-accumulation of zSmad1 in the regions where such an increment was noticeable for zSmad5. Although rather preliminary, our data on

zSmad1 indicates a novel function of zSmad1. The nucleus-localization of zSmad1 might be due to its intrinsic molecular property which differs from zSmad5. Such localization might be caused by interaction with other cellular partner with novel biological activity. Further investigation will be in demand to explain the distinct zSmad1 localization and its function *in vivo*. Because of the predominant nucleus-localization of zSmad1, we could not exclude the possible insensitiveness of the calculation due to the high noise effect.

In short, although our result with zSmad5 argues an involvement of zSmad5 during BMP signal at zebrafish gastrulation, we could not assign zSmad1's function.

3.3 Distinct utilization of Smad proteins in BMP-4 induced myogenic-osteogenic conversion

The pluripotent mesenchymal C2C12 mouse cell line is BMP-sensitive (Blau et al, 1985; Yaffe & Saxel, 1977; Zilberberg et al, 2007) and has been employed in several studies to investigate BMP/Smad signaling (Gromova et al, 2007; Kawai et al, 2000; Nishimura et al, 1998; Yamamoto et al, 1997; Ying et al, 2003). Moreover, BMP was shown to be able to convert the myogenic differentiation of these cells to osteogenic differentiation (Katagiri et al, 1994; Nojima et al, 2010). This cell line thus represents an ideal model system to investigate the functional differences between R-Smads, where a clearly defined stimulus instructs a switch of two distinct differentiation processes. We employed RNA interference to specifically knock down individual Smads, alone or in combination. We examined the effect of Smad silencing on the BMP-4 directed myogenic-osteogenic conversion of C2C12 cells. Our results reveal that different Smads function both in cooperative and in independent manner in BMP signaling.

3.3.1 Expression of endogenous BR-Smads in C2C12 cells and their knockdown

To gain an overview of the endogenous expression of all BR-Smads, we measured their mRNA levels in C2C12 cells by reverse-transcription PCR (RT-PCR). We detected all

mRNAs encoding Smad1, Smad4, Smad5 and Smad8. Smad8 mRNA was present at much lower level than other three (Figure 28A). We further analyzed the abundance of each protein by immuno-blotting (IB) (Figure 28B). The detected expression of all Smads correlated with their mRNA levels. Smad1, Smad4 and Smad5 were expressed at similar levels, while Smad8 level was again significantly lower. A high background was observed in immune-blotting of Smad8 because of its extremely low expression. Treatment with specific siRNA led to significant reduction of expression of each endogenous Smad in both protein and mRNA levels (Figure 28C and D).

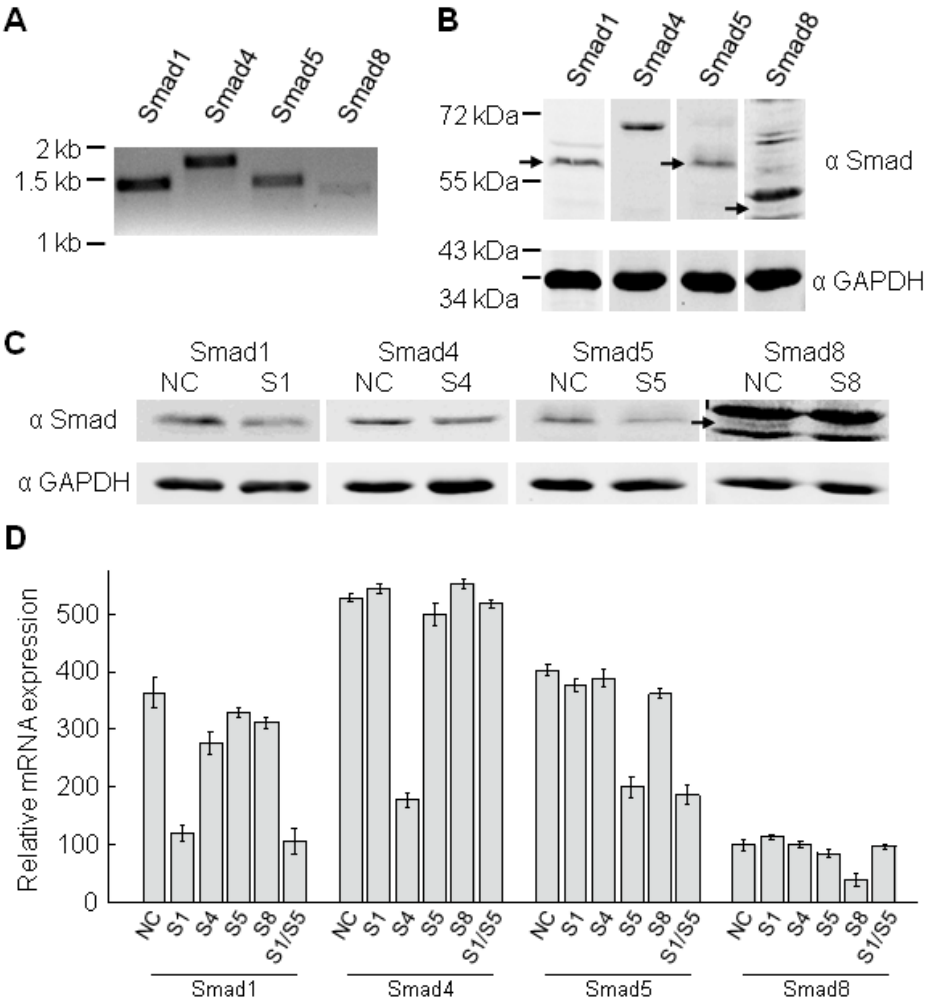

Figure 28: Endogenous expression and knockdown of BMP-regulated Smads in C2C12 cells. (A) Expression of endogenous Smad mRNAs. Full-length cDNA pool was synthesized from total RNA extract using an oligo-dT primer and subjected to reverse-transcription-PCR using gene-specific primer-pairs. The PCR products were resolved by agarose gel

electrophoresis. (B) Expression of endogenous Smad proteins. Lysate corresponding 2x105 cells was subjected for SDS-PAGE following immuno-blotting against individual Smads. GAPDH was applied as internal loading control. Arrows indicated target protein bands. A high background was observed in immune-blotting of Smad8 because of its extremely low expression. (C) Knockdown of endogenous Smad proteins. Cells were treated with specific siRNA as indicated. After 24 hours, cell lysates were prepared and analyzed as in (B). (D) mRNA expression in knockdowns. Cells were treated with specific siRNA as indicated. After 24 hours, total RNA was extracted and cDNA was synthesized. Quantitative real-time PCR was performed with gene-specific primer pairs as decribed in Material and Method. Relative mRNA level was first normalized with GAPDH and scaled to that of Smad8.NC: negative control; S1, S4, S5, S8: siRNA targeting Smad1, Smad4, Smad5, Smad8.

3.3.2 Phosphorylation and nuclear translocation of BR-Smads

To validate the subjection of the BR-Smads to canonical signaling pathway, we investigated their phopsphorylation status and nucleo-translocation following BMP stimulation. Because of their extremely high sequence homology, an appropriate antibody has not yet been available to both distinguish each BR-Smad and recognize the phosphorylated motif. We thus sought to investigate these events with over-expressed recombinant protein constructs. Fusion proteins with an N-terminal green fluorescent protein (GFP) tag were constructed and used to transfect cells. Cells were serum-starved and stimulated by addition of BMP-4. Phosphorylation of the tagged BR-Smads was determined by immuno-staining against phospho-Smad1/5/8 (p-Smad) antibody. Over-expressed GFP-BR-Smads were observed to be phosphorylated under BMP-4 stimulation without exception (Figure 29, compare B and C, E and F, H and I).

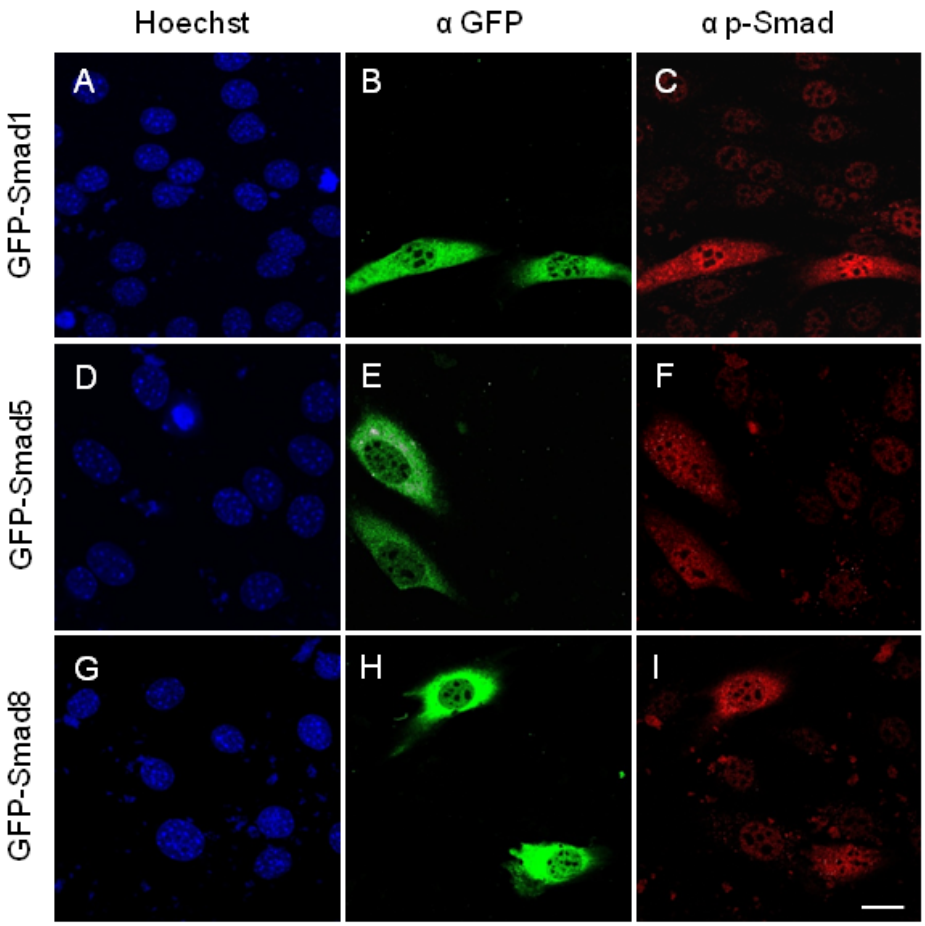

Figure 29: Phosphorylation and nucleo-translocation of over-expressed Smads upon BMP-4 stimulation. C2C12 cells on glass cover slips were transiently transfected with plasmids encoding different meGFP-Smad fusions as indicated in GM. 24 hours post transfection, cells were serum-starved for 16 hours, treated with BMP-4 for 1 hour, fixed and immuno-stained against DNA (Hoechst, blue), p-Smad (red) and GFP (green). Images were acquired on a Leica TCS SP5 confocal microscope with HCX PL APO CS 40.0x1.25 OIL UV objective. Bar: 20 µm

Nuclear translocation of GFP-BR-Smads was evaluated by the increase of nuclear p-Smad staining in transfected cells, as compared to neighbor untransfected cells. Such an increase of nuclear p-Smad staining was observed in all three BR-Smad fusions, suggesting they all undergo cytoplasm-nucleus translocation upon BMP-4 stimulated phosphorylation (Figure 29C, F, I). This result is in agreement with previous observations

and indicates that the BMP signal is equitably allocated to all its downstream transmitters (Gromova et al, 2007; Kawai et al, 2000; Yamamoto et al, 1997).

3.3.3 Involvement of BR-Smads in BMP-dependent inhibition of myogenesis

Both TGF-β and BMP have been shown to be able to inhibit the myogenic differentiation of C2C12 cells (Katagiri et al, 1994; Olson et al, 1986) and the former was believed to mediated by Smad3 (Liu et al, 2001). To investigate the utility of BR-Smads in BMP-directed inhibition event, we used RNA interference (RNAi) to specifically knock down individual endogenous BR-Smad and assayed the effect of Smad silencing on BMP directed myogenic inhibition. Myogenic differentiation of C2C12 cells was determined by positive immuno-staining for the myosin heavy chain.

After we re-cultured the cells in differentiation medium, we observed a noticeable population of myosin-positive cells, which was significantly inhibited by the addition and presence of BMP-4 (Figure 30A, B, J). The knockdown of Smad4 caused a substantial recovery to 96% of the myosin-positive cell population in the presence of BMP-4 (Figure 30D, J). This result indicates that the myogenic inhibition is Smad-dependent. To further search for the relevant BR-Smads, single and double knockdowns of BR-Smads were performed. Surprisingly only the simultaneous knockdown of Smad1 and Smad5 was capable of reducing the myogenic inhibition of BMP-4 with 98% MHC-positive cell population in a manner comparable to that of Smad4 silencing (Figure 30G, J). The knockdown of Smad1, Smad5 or Smad8 alone, or double knockdown of Smad1/8 or Smad5/8 did not prevent BMP-4 inhibition of myogenic differentiation (Figure 30C, E, F, H, I, J).

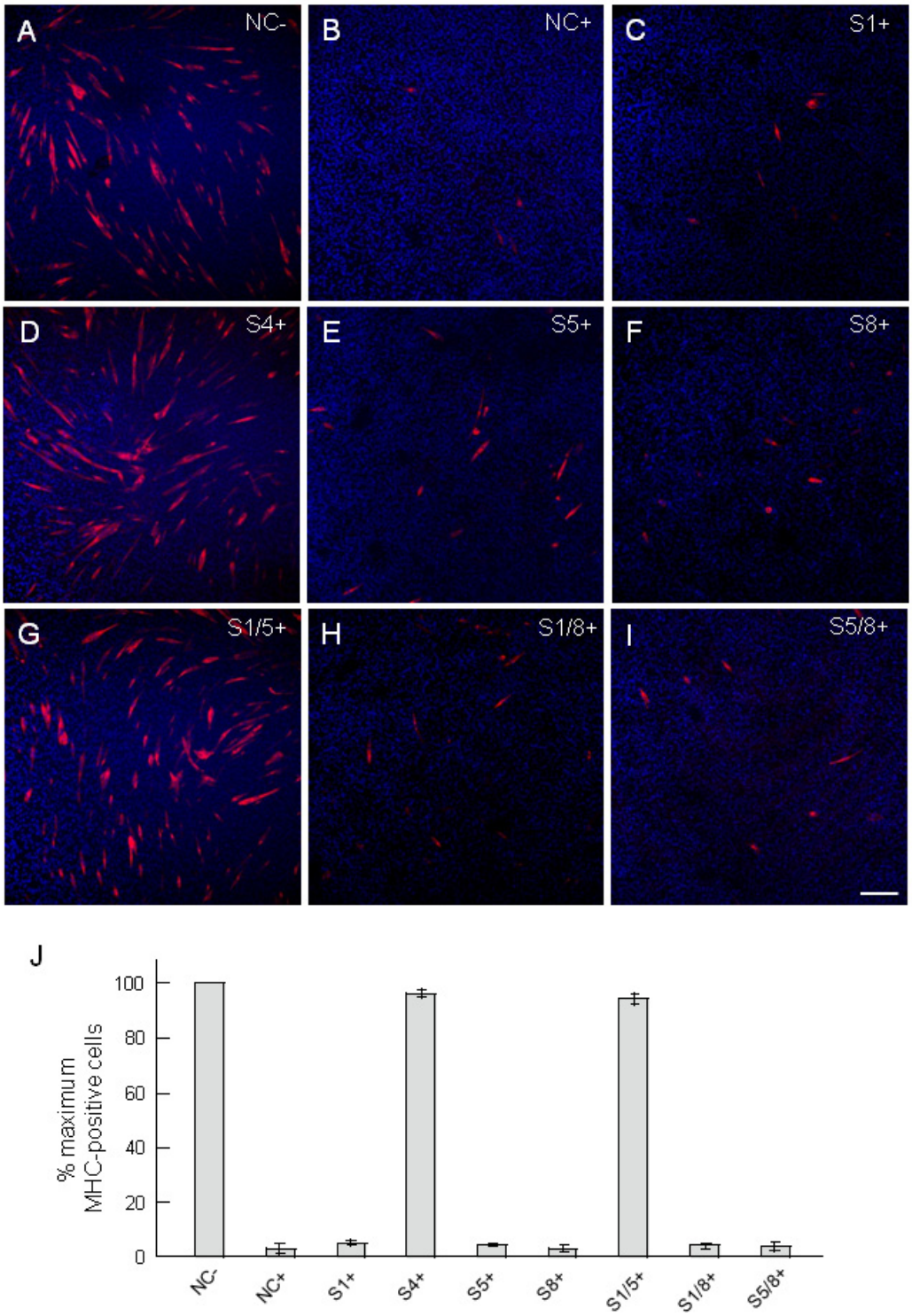

Figure 30: Redundant Smad function in myogenesis. C2C12 cells grown on glass coverslips were treated with specific siRNAs as indicated in GM. After 24 hours, medium was replaced with DM with BMP-4 for 3 h and then removed by re-culturing with fresh DM without BMP-4. On day 4, cells were fixed with PFA, followed by immuno-staining against DNA (Hoechst, blue) and myosin heavy chain (red). (A)-(F), effects of single knockdowns on myogenic

inhibition. (G)-(I), effects of double knockdown. Representative images were from one out of three independent experiments with similar results acquired on a Leica TCS SP5 confocal microscope with HC PL FLUOTAR 10.0x0.30 DRY objective. Bar: 200 μm (J), enumerated summary of three repetitive experiments. MHC-positive cells on coverslips were counted and the effect of Smad silencing on myogenic inhibition was enumerated by the percent ratio of MHC-positive cell number of each Smad knockdown to that of negative control in absence of BMP-4. Values were mean ± standard error.

These observations demonstrate that Smad1 or Smad5 can individually mediate the BMP-4 signal that inhibits myogenic differentiation indicating their functional redundancy in this process. Smad8, in contrast, had no involvement in this process.

3.3.4 Involvement of BR-Smads in BMP induction of osteogenesis

We then investigated the function of BR-Smads in BMP induced osteoblast differentiation. Activity of alkaline phosphatase (ALP), an osteoblast marker, was employed as a measure of osteoblast differentiation following addition of BMP-4. The single knockdown of Smad4 significantly reduced the ALP positive cell population to 27% (Figure 31D, G), demonstrating that this BMP-dependent function is also Smad-dependent.

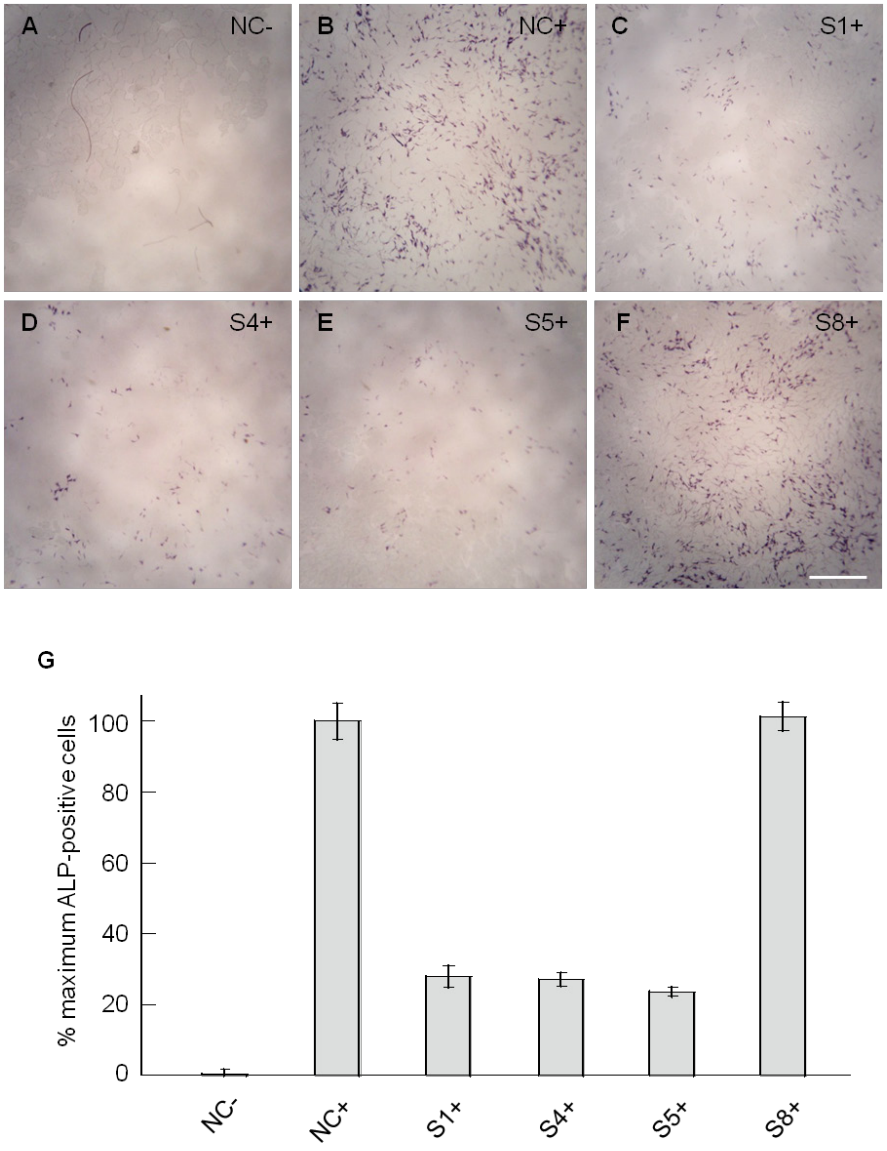

Figure 31: Cooperative Smad function in osteogenesis. C2C12 cells grown on glass coverslips were treated with specific siRNA as indicated in GM. After 24 hours, medium was replaced with DM with BMP-4 and replaced every day. On day 4, cells were fixed with PFA and osteoblasts (blue) were stained for ALP activity. (A)-(F), effects of single knockdowns on osteoblastic induction. Representative images of one experiment were taken with digital camera through the ocular of an ordinary bench stereomicroscope. Bar: 1 mm (G), enumerated summary of three repetitive experiments. ALP-positive cells on coverslips were counted and the effect of Smad silencing on osteoblast

induction was enumerated by the percent ratio of ALP-positive cell number of each Smad knockdown to that of negative control in presence of BMP-4. Values were mean ± standard error. -: without BMP-4; +: with BMP-4; NC: negative control; S1, S4, S5, S8: siRNA targeting Smad1, Smad4, Smad5, Smad8.

The individual knockdowns of Smad1, Smad5 and Smad8 had different outcomes. Knockdown of either Smad1 or Smad5 caused a significant reduction in ALP-positive cells with 28% and 24% respectively (Figure 31C, D, and G). Such effects were comparable to that observed after Smad4 silencing (Figure 31E, G). The loss of Smad8 had no effect on C2C12 differentiation (Figure 31F, G). These results confirm that both Smad1 and Smad5 are involved in BMP-4 induced osteoblast differentiation in a cooperative manner, as reported in previous studies (Nojima et al, 2010; Yamamoto et al, 1997).

3.3.5 Interaction between Smad proteins and pathway-specific regulators

Although both Smad1 and Smad5 were involved in myogenesis and in osteogenesis, the manner how they were involved seemed novel based on the results above. Interestingly, both activities were acquired for sake of ALP whereas either of them could inhibit MHC. Therefore, we were interested to investigate the interaction between Smad protein and pathway-specific regulators to gain more insight to the molecular mechanism behind.

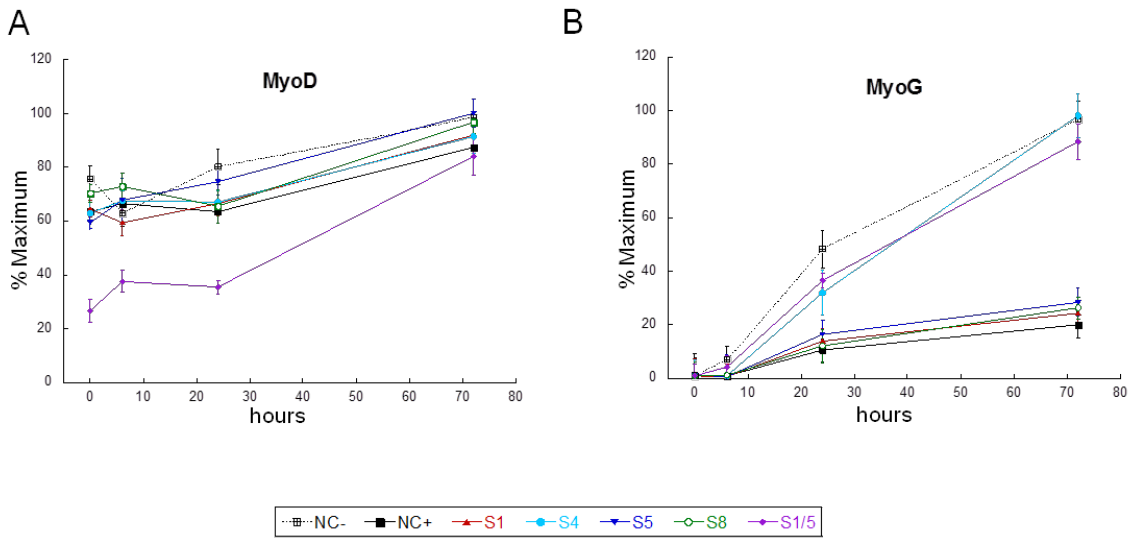

Figure 32: mRNA expression profile of MyoD and MyoG in BMP-treated C2C12 cells with different Smad knockdowns. Cells were first treated with specific siRNA as indicated for 24 hours and then exposed to BMP-4 stimulation for 2 hours and re-cultured in DM for up to 3 days. Total RNA was extracted from cells harvested at different time-points after BMP-stimulation as indicated. cDNA was synthesized and quantitative real-time PCR was performed with gene-specific primer pairs as described in Material and Method. mRNA level was normalized with GAPDH and n=3 assays per time-point were plotted. -: without BMP-4; +: with BMP-4; NC: negative control; S1, S4, S5, S8: siRNA targeting Smad1, Smad4, Smad5, Smad8.

We assayed the expression dynamics of MyoD (Davis et al, 1987; Komaki et al, 2004) and MyoG (Wright et al, 1989) as myogenic regulators in our Smad-knockdowns. A modest, relatively steady expression of MyoD was observed in cells irrespective of BMP treatment (Figure 32A, NC- and NC+). Such expression was not affected by any of the single knockdowns (Figure 32A). Nevertheless, we did observe a drop of the initial expression of MyoD in the double knockdown of S1/5, which made up to the same level at with others gradually (Figure 32A). MyoG on the contrary, was only inducibly expressed in absence of BMP (Figure 32B, NC-). Addition of BMP led to a significant drop of its expression by 80% (Figure 32B, NC+). Such inhibition was not affected in

single knockdowns of S1, S5 or S8, but was reversed in single knockdown of S4 or double knockdown of S1/5 (Figure 32B). Such observation was in agreement with the results obtained with MHC staining above, indicating that either Smad1 or Smad5 could inhibit the MyoG independently and it did so in fact.

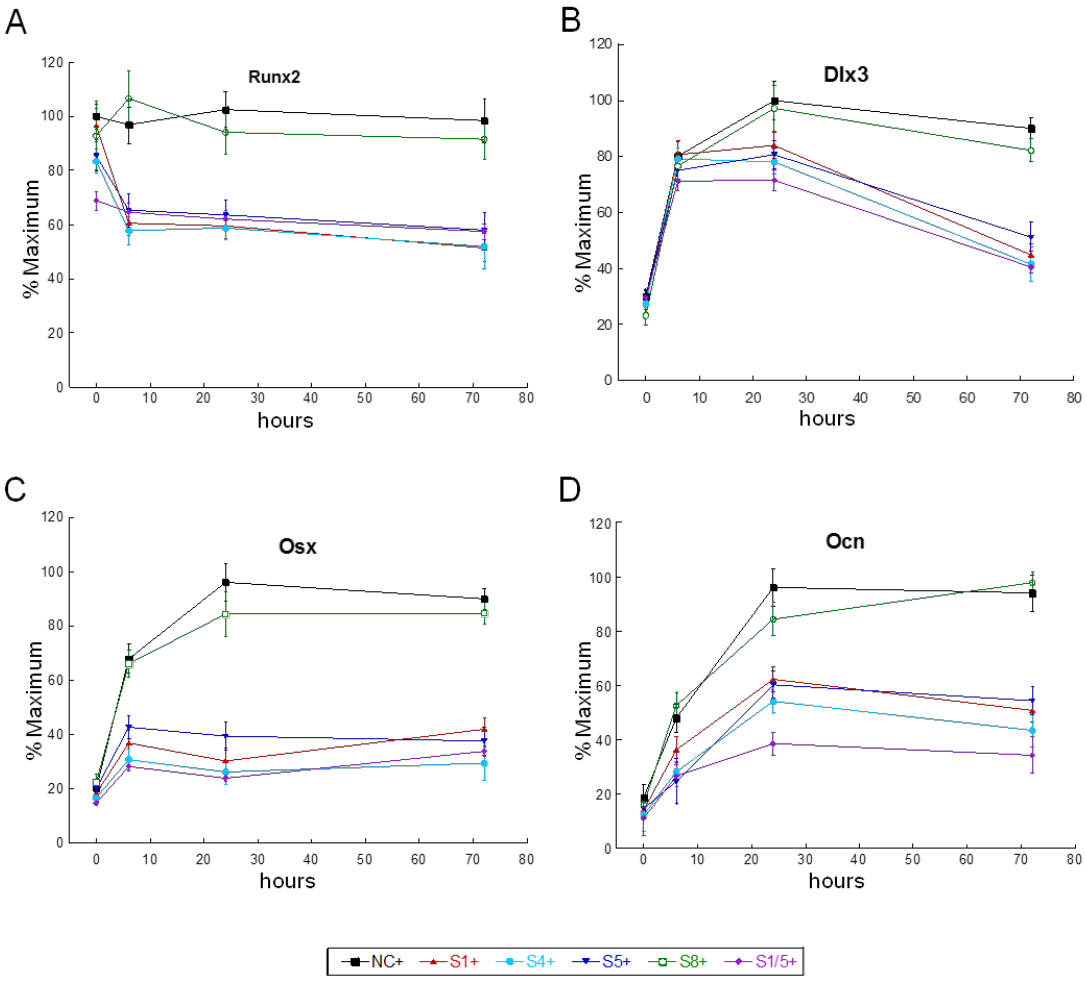

Figure 33: mRNA profile of Runx2, Dlx3, Osx and Ocn in BMP-treated C2C12 cells with different Smad knockdowns. Cells were first treated with specific siRNA as indicated for 24 hours and then re-cultured in DM supplemented with BMP-4 for up to 3 days with daily refreshment. Total RNA was extracted from cells harvested at different time-points after BMP-stimulation as indicated. cDNA was synthesized and quantitative real-time PCR was performed with gene-specific primer pairs as described in Material and Method. mRNA level was normalized with GAPDH and n=3 assays per time-point were plotted. +: with BMP-4; NC: negative control; S1, S4, S5, S8: siRNA targeting Smad1, Smad4, Smad5, Smad8.

We also investigate the effects of Smad knockdowns on osteogenic regulators, such as Runx2 (Ducy et al, 1997), Dlx3 (Hassan et al, 2004) and Osx (Osterix) (Nakashima et al, 2002) as well as the Ocn (Osteocalcin) as another osteoblast marker. Runx2 was steadily expressed in C2C12 cells and addition of BMP did not result a noticeable change on its level (Figure 33A, NC+). A reduction of Runx2 was observed with the loss of Smad1, Smad4 or Smad5 alone except Smad8 (Figure 33A). Meanwhile, Dlx3, Osx and Ocn were all inducibly expressed by BMP (Figure 33A, B, C and D). Similar to that with Runx2, the induction of these genes were significantly impaired in absence of Smad1, Smad4 or Smad5 alone. By 72 hours post induction, an average of 50% loss of mRNA was observed for Runx2, Dlx3 and Ocn while almost 60% loss for Osx. These observations were in concert with the ALP staining regarding individual knockdown setups.

3.3.6 Conclusion

In summary, the vast range of biological responses instructed by BMPs in multiple-cellular organisms converges upon three highly conserved BR-Smads. How each Smad functionally contributes to signal transduction that affects multiple cellular responses has been a question of long-standing interest for investigators in various disciplines. We investigated the functional differences among these Smads in the context of BMP-4 directed myogenic-osteoblastic conversion of C2C12 cells (Ryoo et al, 2006).

We found evidence for both redundant and non-redundant functions of Smad1 and Smad5. Both Smad1 and Smad5 were observed to be essential for transmitting BMP's signal to promote the osteogenesis. Loss of either of them impaired the process significantly and loss of both enhanced the impairment. Such impairment was further validated to be the result of the coherently affected osteogenic regulators. Inhibition of myogenesis on the other hand could be independently mediated by either Smad1 or Smad5, as not only the MHC as terminal marker but MyoD and MyoG as intermediate regulators were exclusively not affected till both transmitters were down-regulated.

Receptor-phosphorylated, active Smad proteins are believed to form heteromeric complex with Smad4 as functional transcription factor activity (Massague et al, 2005; ten Dijke & Hill, 2004). Heterotrimeric complexes of Smad4 with Smad2 and/or Smad3 have been reported in numerous previous studies on TGF-β signaling pathway (Inman & Hill, 2002). Due to the homology of these proteins and conservation of the signaling pathway, BMP-Smads might also form distinct complexes so as to perform their specific roles (Feng & Derynck, 2005). We argue therefore, that a Smad1/Smad5/Smad4 complex is responsible for promoting the osteoblast and this complex is essential for multiple sequential steps during the differentiation (Figure 34, yellow). Myogenic inhibition in contrast could be transmitted by many other complex constitutions such as heterodimer of Smad4 and Smad1 or Smad5, heterotrimer of Smad4 and two copies of Smad1 or Smad5 (Figure 34, magenta). Such speculation might also help explain the fact that myogenesis is readily inhibited by BMP treatment for only up to 2 hrs at the beginning due to the enrichment of multiple inhibiting complexes comparing to the osteogenic conversion which is in need of continuous BMP induction for days. Therefore, utilization of distinct Smad complexes might be responsible for BMP to specify its downstream cellular responses. The phenotypes of Smad1 knockout mice were observed to be similar to those in Smad5 knockout mice in previous studies (Arnold et al, 2006; Chang et al, 1999; Tremblay et al, 2001). It might be possible that the loss of either of them failed to form a functional Smad1/Smad5/Smad4 heteromeric complex, which might be the active signal transmitter for the specified pathways as proposed in our osteogenesis-promoting model. Nevertheless, direct evidence of existence of such complexes as well as their functional characterization would be desirable for validation.

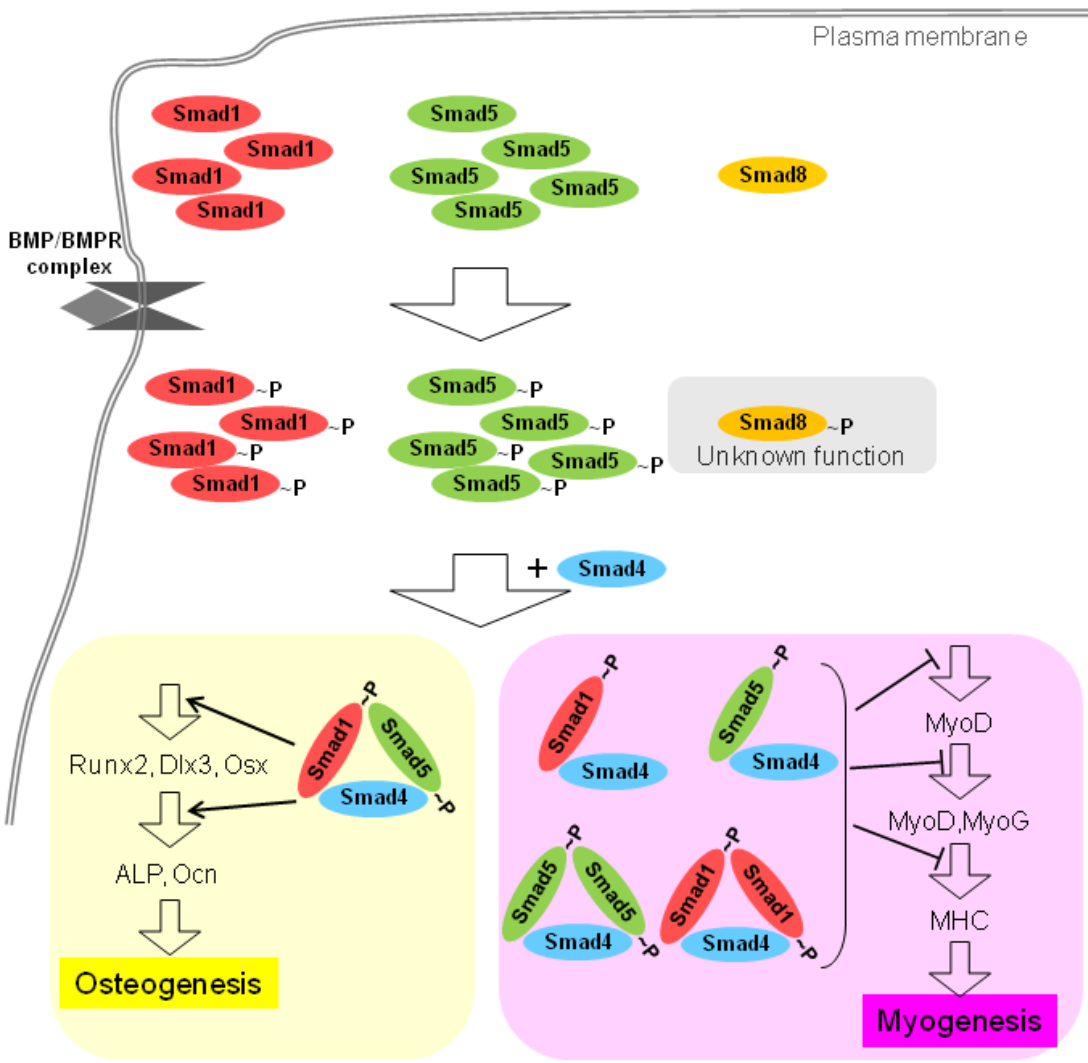

Figure 34: Hypothetic Smad complexes involved in C2C12 myogenic-osteogenic conversion. Smad proteins are phosphorylated upon BMP stimulation and form different stoichiometric complexes, which perform distinct cellular functions. The Smad4/Smad1/Smad5 heterotrimer might be responsible for osteoblast promotion (yellow). Heterodimer of Smad4/Smad1 or Smad4/Smad5 as well as heterotrimer of Smad4/Smad1/Smad1 or Smad4/Smad5/Smad5 might be essential for inhibiting myogenic differentiation (magenta).

Although our conclusions are based on the study of a simplified system, their implications could be relevant in a wider context because BMP-4 is the most universal developmental regulator, and Smad1 and Smad5 are ubiquitously expressed throughout early stage of mouse development (Arnold et al, 2006; Chang et al, 1999; Hogan, 1996; Tremblay et al, 2001). To our knowledge, our data contributes as an initial, if not the first, evidence on

stoichiometric study of BMP-Smads regarding two biological events. We hence provide a glance at functional complexity of the division of Smad functions, and constitute a basis, on which in-depth studies of BMP/Smad signaling can be initiated to elucidate the intricacies of this key signaling pathway.

4 References

Ai HW, Shaner NC, Cheng Z, Tsien RY, Campbell RE (2007) Exploration of new chromophore structures leads to the identification of improved blue fluorescent proteins. *Biochemistry* **46:** 5904-5910

Ando R, Hama H, Yamamoto-Hino M, Mizuno H, Miyawaki A (2002) An optical marker based on the UV-induced green-to-red photoconversion of a fluorescent protein. *Proc Natl Acad Sci U S A* **99:** 12651-12656

Arnold SJ, Maretto S, Islam A, Bikoff EK, Robertson EJ (2006) Dose-dependent Smad1, Smad5 and Smad8 signaling in the early mouse embryo. *Dev Biol* **296:** 104-118

Baba T, Ara T, Hasegawa M, Takai Y, Okumura Y, Baba M, Datsenko KA, Tomita M, Wanner BL, Mori H (2006) Construction of *Escherichia coli* K-12 in-frame, single-gene knockout mutants: the Keio collection. *Mol Syst Biol* **2:** 2006 0008

Balciunas D, Wangensteen KJ, Wilber A, Bell J, Geurts A, Sivasubbu S, Wang X, Hackett PB, Largaespada DA, McIvor RS, Ekker SC (2006) Harnessing a high cargo-capacity transposon for genetic applications in vertebrates. *PLoS Genet* **2:** e169

Beis D, Stainier DY (2006) In vivo cell biology: following the zebrafish trend. *Trends Cell Biol* **16:** 105-112

Blau HM, Pavlath GK, Hardeman EC, Chiu CP, Silberstein L, Webster SG, Miller SC, Webster C (1985) Plasticity of the differentiated state. *Science* **230:** 758-766

Chang H, Huylebroeck D, Verschueren K, Guo Q, Matzuk MM, Zwijsen A (1999) Smad5 knockout mice die at mid-gestation due to multiple embryonic and extraembryonic defects. *Development* **126:** 1631-1642

Chen D, Zhao M, Mundy GR (2004) Bone morphogenetic proteins. *Growth Factors* **22:** 233-241

Collery RF, Link BA (2011) Dynamic smad-mediated BMP signaling revealed through transgenic zebrafish. *Dev Dyn* **240:** 712-722

Collins TJ (2007) ImageJ for microscopy. *Biotechniques* **43:** 25-30

Cormack BP, Valdivia RH, Falkow S (1996) FACS-optimized mutants of the green fluorescent protein (GFP). *Gene* **173:** 33-38

Davis-Dusenbery BN, Hata A (2011) Smad-mediated miRNA processing: a critical role for a conserved RNA sequence. *RNA Biol* **8:** 71-76

Davis BN, Hilyard AC, Lagna G, Hata A (2008) SMAD proteins control DROSHA-mediated microRNA maturation. *Nature* **454:** 56-61

Davis RL, Weintraub H, Lassar AB (1987) Expression of a single transfected cDNA converts fibroblasts to myoblasts. *Cell* **51:** 987-1000

Derynck R, Zhang YE (2003) Smad-dependent and Smad-independent pathways in TGF-beta family signalling. *Nature* **425:** 577-584

Dick A, Meier A, Hammerschmidt M (1999) Smad1 and Smad5 have distinct roles during dorsoventral patterning of the zebrafish embryo. *Dev Dyn* **216:** 285-298

Ducy P, Zhang R, Geoffroy V, Ridall AL, Karsenty G (1997) Osf2/Cbfa1: a transcriptional activator of osteoblast differentiation. *Cell* **89:** 747-754

Feng XH, Derynck R (2005) Specificity and versatility in tgf-beta signaling through Smads. *Annu Rev Cell Dev Biol* **21:** 659-693

Friedrich M (2009) Untersuchung zur Verbesserung der axialen Auflösung eines SPIM-Mikroskops durch stimulierte Abregung der Fluoreszenz (engl. STED). *Diplomarbeit TU Illmenau***:** 120

Graham FL, Smiley J, Russell WC, Nairn R (1977) Characteristics of a human cell line transformed by DNA from human adenovirus type 5. *J Gen Virol* **36:** 59-74

Gromova KV, Friedrich M, Noskov A, Harms GS (2007) Visualizing Smad1/4 signaling response to bone morphogenetic protein-4 activation by FRET biosensors. *Biochim Biophys Acta* **1773:** 1759-1773

Gurskaya NG, Verkhusha VV, Shcheglov AS, Staroverov DB, Chepurnykh TV, Fradkov AF, Lukyanov S, Lukyanov KA (2006) Engineering of a monomeric green-to-red photoactivatable fluorescent protein induced by blue light. *Nat Biotechnol* **24:** 461-465

Harradine KA, Akhurst RJ (2006) Mutations of TGFbeta signaling molecules in human disease. *Ann Med* **38:** 403-414

Hassan MQ, Javed A, Morasso MI, Karlin J, Montecino M, van Wijnen AJ, Stein GS, Stein JL, Lian JB (2004) Dlx3 transcriptional regulation of osteoblast differentiation: temporal recruitment of Msx2, Dlx3, and Dlx5 homeodomain proteins to chromatin of the

osteocalcin gene. *Mol Cell Biol* **24:** 9248-9261

Heldin CH, Miyazono K, ten Dijke P (1997) TGF-beta signalling from cell membrane to nucleus through SMAD proteins. *Nature* **390:** 465-471

Hogan BL (1996) Bone morphogenetic proteins: multifunctional regulators of vertebrate development. *Genes Dev* **10:** 1580-1594

Inman GJ, Hill CS (2002) Stoichiometry of active smad-transcription factor complexes on DNA. *J Biol Chem* **277:** 51008-51016

Johnson AD, Krieg PA (1994) pXeX, a vector for efficient expression of cloned sequences in Xenopus embryos. *Gene* **147:** 223-226

Jonk LJ, Itoh S, Heldin CH, ten Dijke P, Kruijer W (1998) Identification and functional characterization of a Smad binding element (SBE) in the JunB promoter that acts as a transforming growth factor-beta, activin, and bone morphogenetic protein-inducible enhancer. *J Biol Chem* **273:** 21145-21152

Katagiri T, Yamaguchi A, Komaki M, Abe E, Takahashi N, Ikeda T, Rosen V, Wozney JM, Fujisawa-Sehara A, Suda T (1994) Bone morphogenetic protein-2 converts the differentiation pathway of C2C12 myoblasts into the osteoblast lineage. *J Cell Biol* **127:** 1755-1766

Kawai S, Faucheu C, Gallea S, Spinella-Jaegle S, Atfi A, Baron R, Roman SR (2000) Mouse smad8 phosphorylation downstream of BMP receptors ALK-2, ALK-3, and ALK-6 induces its association with Smad4 and transcriptional activity. *Biochem Biophys Res Commun* **271:** 682-687

Kawakami K (2007) Tol2: a versatile gene transfer vector in vertebrates. *Genome Biol* **8 Suppl 1:** S7

Keller PJ, Schmidt AD, Wittbrodt J, Stelzer EH (2008) Reconstruction of zebrafish early embryonic development by scanned light sheet microscopy. *Science* **322:** 1065-1069

Keller PJ, Schmidt AD, Wittbrodt J, Stelzer EH (2011) Digital Scanned Laser Light-Sheet Fluorescence Microscopy (DSLM) of Zebrafish and Drosophila Embryonic Development. *Cold Spring Harb Protoc* **2011**

Kimmel CB, Ballard WW, Kimmel SR, Ullmann B, Schilling TF (1995) Stages of embryonic development of the zebrafish. *Dev Dyn* **203:** 253-310

Komaki M, Asakura A, Rudnicki MA, Sodek J, Cheifetz S (2004) MyoD enhances

BMP7-induced osteogenic differentiation of myogenic cell cultures. *J Cell Sci* **117:** 1457-1468

Korchynskyi O, ten Dijke P (2002) Identification and functional characterization of distinct critically important bone morphogenetic protein-specific response elements in the Id1 promoter. *J Biol Chem* **277:** 4883-4891

Laux DW, Febbo JA, Roman BL (2011) Dynamic analysis of BMP-responsive smad activity in live zebrafish embryos. *Dev Dyn* **240:** 682-694

Liu D, Black BL, Derynck R (2001) TGF-beta inhibits muscle differentiation through functional repression of myogenic transcription factors by Smad3. *Genes Dev* **15:** 2950-2966

Maegawa S, Varga M, Weinberg ES (2006) FGF signaling is required for {beta}-catenin-mediated induction of the zebrafish organizer. *Development* **133:** 3265-3276

Massague J, Seoane J, Wotton D (2005) Smad transcription factors. *Genes Dev* **19:** 2783-2810

McReynolds LJ, Gupta S, Figueroa ME, Mullins MC, Evans T (2007) Smad1 and Smad5 differentially regulate embryonic hematopoiesis. *Blood* **110:** 3881-3890

Miyazono K, Kamiya Y, Morikawa M (2010) Bone morphogenetic protein receptors and signal transduction. *J Biochem* **147:** 35-51

Nakashima K, Zhou X, Kunkel G, Zhang Z, Deng JM, Behringer RR, de Crombrugghe B (2002) The novel zinc finger-containing transcription factor osterix is required for osteoblast differentiation and bone formation. *Cell* **108:** 17-29

Nishimura R, Kato Y, Chen D, Harris SE, Mundy GR, Yoneda T (1998) Smad5 and DPC4 are key molecules in mediating BMP-2-induced osteoblastic differentiation of the pluripotent mesenchymal precursor cell line C2C12. *J Biol Chem* **273:** 1872-1879

Nojima J, Kanomata K, Takada Y, Fukuda T, Kokabu S, Ohte S, Takada T, Tsukui T, Yamamoto TS, Sasanuma H, Yoneyama K, Ueno N, Okazaki Y, Kamijo R, Yoda T, Katagiri T (2010) Dual roles of smad proteins in the conversion from myoblasts to osteoblastic cells by bone morphogenetic proteins. *J Biol Chem* **285:** 15577-15586

Olson EN, Sternberg E, Hu JS, Spizz G, Wilcox C (1986) Regulation of myogenic differentiation by type beta transforming growth factor. *J Cell Biol* **103:** 1799-1805

Pangas SA, Li X, Umans L, Zwijsen A, Huylebroeck D, Gutierrez C, Wang D, Martin JF,

Jamin SP, Behringer RR, Robertson EJ, Matzuk MM (2008) Conditional deletion of Smad1 and Smad5 in somatic cells of male and female gonads leads to metastatic tumor development in mice. *Mol Cell Biol* **28:** 248-257

Rozen S, Skaletsky H (2000) Primer3 on the WWW for general users and for biologist programmers. *Methods Mol Biol* **132:** 365-386

Ryoo HM, Lee MH, Kim YJ (2006) Critical molecular switches involved in BMP-2-induced osteogenic differentiation of mesenchymal cells. *Gene* **366:** 51-57

Sambrook J, Russell DW (2006) *The condensed protocols from molecular cloning : a laboratory manual*, Cold Spring Harbor, N.Y.: Cold Spring Harbor Laboratory Press.

Schmierer B, Hill CS (2007) TGFbeta-SMAD signal transduction: molecular specificity and functional flexibility. *Nat Rev Mol Cell Biol* **8:** 970-982

Shaner NC, Campbell RE, Steinbach PA, Giepmans BN, Palmer AE, Tsien RY (2004) Improved monomeric red, orange and yellow fluorescent proteins derived from Discosoma sp. red fluorescent protein. *Nat Biotechnol* **22:** 1567-1572

Singh A, Morris RJ (2010) The Yin and Yang of bone morphogenetic proteins in cancer. *Cytokine Growth Factor Rev* **21:** 299-313

Song B, Estrada KD, Lyons KM (2009) Smad signaling in skeletal development and regeneration. *Cytokine Growth Factor Rev* **20:** 379-388

Spandidos A, Wang X, Wang H, Seed B (2010) PrimerBank: a resource of human and mouse PCR primer pairs for gene expression detection and quantification. *Nucleic Acids Res* **38:** D792-799

Studier FW, Moffatt BA (1986) Use of bacteriophage T7 RNA polymerase to direct selective high-level expression of cloned genes. *J Mol Biol* **189:** 113-130

Szymczak AL, Vignali DA (2005) Development of 2A peptide-based strategies in the design of multicistronic vectors. *Expert Opin Biol Ther* **5:** 627-638

Szymczak AL, Workman CJ, Wang Y, Vignali KM, Dilioglou S, Vanin EF, Vignali DA (2004) Correction of multi-gene deficiency in vivo using a single 'self-cleaving' 2A peptide-based retroviral vector. *Nat Biotechnol* **22:** 589-594

Taylor RG, Walker DC, McInnes RR (1993) E. coli host strains significantly affect the quality of small scale plasmid DNA preparations used for sequencing. *Nucleic Acids Res* **21:** 1677-1678

ten Dijke P, Hill CS (2004) New insights into TGF-beta-Smad signalling. *Trends Biochem Sci* **29:** 265-273

Thawani JP, Wang AC, Than KD, Lin CY, La Marca F, Park P (2010) Bone morphogenetic proteins and cancer: review of the literature. *Neurosurgery* **66:** 233-246; discussion 246

Thisse B, Heyer V, Lux A, Alunni V, Degrave A, Seiliez I, Kirchner J, Parkhill JP, Thisse C (2004) Spatial and temporal expression of the zebrafish genome by large-scale in situ hybridization screening. *Methods Cell Biol* **77:** 505-519

Toramoto T, Ikeda D, Ochiai Y, Minoshima S, Shimizu N, Watabe S (2004) Multiple gene organization of pufferfish Fugu rubripes tropomyosin isoforms and tissue distribution of their transcripts. *Gene* **331:** 41-51

Tremblay KD, Dunn NR, Robertson EJ (2001) Mouse embryos lacking Smad1 signals display defects in extra-embryonic tissues and germ cell formation. *Development* **128:** 3609-3621

Tucker JA, Mintzer KA, Mullins MC (2008) The BMP signaling gradient patterns dorsoventral tissues in a temporally progressive manner along the anteroposterior axis. *Dev Cell* **14:** 108-119

Urasaki A, Morvan G, Kawakami K (2006) Functional dissection of the Tol2 transposable element identified the minimal cis-sequence and a highly repetitive sequence in the subterminal region essential for transposition. *Genetics* **174:** 639-649

Urist MR (1965) Bone: formation by autoinduction. *Science* **150:** 893-899

Varga AC, Wrana JL (2005) The disparate role of BMP in stem cell biology. *Oncogene* **24:** 5713-5721

Watabe T, Miyazono K (2009) Roles of TGF-beta family signaling in stem cell renewal and differentiation. *Cell Res* **19:** 103-115

Wiedenmann J, Ivanchenko S, Oswald F, Schmitt F, Rocker C, Salih A, Spindler KD, Nienhaus GU (2004) EosFP, a fluorescent marker protein with UV-inducible green-to-red fluorescence conversion. *Proc Natl Acad Sci U S A* **101:** 15905-15910

Wootton D (2006) *Bad medicine : doctors doing harm since Hippocrates*, Oxford: Oxford University Press.

Wright WE, Sassoon DA, Lin VK (1989) Myogenin, a factor regulating myogenesis, has a domain homologous to MyoD. *Cell* **56:** 607-617

Yaffe D, Saxel O (1977) Serial passaging and differentiation of myogenic cells isolated from dystrophic mouse muscle. *Nature* **270:** 725-727

Yamamoto N, Akiyama S, Katagiri T, Namiki M, Kurokawa T, Suda T (1997) Smad1 and smad5 act downstream of intracellular signalings of BMP-2 that inhibits myogenic differentiation and induces osteoblast differentiation in C2C12 myoblasts. *Biochem Biophys Res Commun* **238:** 574-580

Ying SX, Hussain ZJ, Zhang YE (2003) Smurf1 facilitates myogenic differentiation and antagonizes the bone morphogenetic protein-2-induced osteoblast conversion by targeting Smad5 for degradation. *J Biol Chem* **278:** 39029-39036

Yuste R (2005) Fluorescence microscopy today. *Nat Methods* **2:** 902-904

Zacharias DA, Violin JD, Newton AC, Tsien RY (2002) Partitioning of lipid-modified monomeric GFPs into membrane microdomains of live cells. *Science* **296:** 913-916

Zilberberg L, ten Dijke P, Sakai LY, Rifkin DB (2007) A rapid and sensitive bioassay to measure bone morphogenetic protein activity. *BMC Cell Biol* **8:** 41

5 Publications

1. Friedrich M, Nozadze R, **Gan Q**, Zelman-Femiak M, Ermolayev V, Wagner TU, Harms GS
   "Detection of single quantum dots in model organisms with sheet illumination microscopy"
   Biochem Biophys Res Commun. 2009 Dec 18; 390(3):722-7

2. Friedrich M, **Gan Q**, Ermolayev V, Harms GS
   "STED-SPIM: Stimulated emission depletion improves sheet illumination microscopy resolution"
   Biophys J. 2011 Apr 20; 100(8):L43-5

3. **Gan Q***, Li H, Zheng PL, Wagner TU, Kissler S, Harms GS*
   *** Correspondence author**
   "Distinct Smad utilization in BMP-4 induced myogenic-osteogenic conversion"
   (Submitted in Journal of Cellular Biochemistry)

6 Affidavit

I hereby confirm that my thesis entitled “Investigation on Distinct Roles of Smad Proteins in Mediating Bone Morphogenetic Proteins Signals” is the results of my own work. I did not receive any help or support from commercial consultants. All sources and/or materials applied are listed and specified in the thesis.

Furthermore, I confirm that this thesis has not been submitted as part of another examination process neither in identical nor in similar form.

Würzburg, Dec 20th, 2011 _____

Place, Date Signature (Gan, Qiang)